Clinical Science (2023) **137** 617–631
https://doi.org/10.1042/CS20220642

Research Article

Repetitive *schistosoma* exposure causes perivascular lung fibrosis and persistent pulmonary hypertension

Rahul Kumar[1,2], Michael H. Lee[1,2], Biruk Kassa[1,2], Dara C. Fonseca Balladares[1,2], Claudia Mickael[3], Linda Sanders[3], Adam Andruska[4], Maya Kumar[5], Edda Spiekerkoetter[4], Angela Bandeira[6], Kurt R. Stenmark[7], Rubin M. Tuder[3] and Brian B Graham[1,2]

[1]Department of Medicine, Division of Pulmonary and Critical Care Medicine, University of California San Francisco, San Francisco, California, U.S.A.; [2]Lung Biology Center, Zuckerberg San Francisco General Hospital, San Francisco, California, U.S.A.; [3]Department of Medicine, Division of Pulmonary Sciences and Critical Care Medicine, University of Colorado Anschutz Medical Campus, Aurora, CO, U.S.A.; [4]Department of Medicine, Division of Pulmonary, Allergy and Critical Care Medicine, Stanford University, Palo Alto, CA, U.S.A.; [5]Department of Pediatrics, Division of Pulmonary Medicine, Stanford University, Palo Alto, CA, U.S.A.; [6]PROCAPE, Universidade de Pernambuco, Recife, Pernambuco, Brazil; [7]Department of Pediatrics, University of Colorado Anschutz Medical Campus, Aurora, CO, U.S.A.

Correspondence: Rahul Kumar (rahul.kumar2@ucsf.edu) or Brian Graham (brian.graham@ucsf.edu)

OPEN ACCESS

Background: Pulmonary hypertension (PH) can occur as a complication of schistosomiasis. In humans, schistosomiasis-PH persists despite antihelminthic therapy and parasite eradication. We hypothesized that persistent disease arises as a consequence of exposure repetition.
Methods: Following intraperitoneal sensitization, mice were experimentally exposed to *Schistosoma* eggs by intravenous injection, either once or three times repeatedly. The phenotype was characterized by right heart catheterization and tissue analysis.
Results: Following intraperitoneal sensitization, a single intravenous *Schistosoma* egg exposure resulted in a PH phenotype that peaked at 7–14 days, followed by spontaneous resolution. Three sequential exposures resulted in a persistent PH phenotype. Inflammatory cytokines were not significantly different between mice exposed to one or three egg doses, but there was an increase in perivascular fibrosis in those who received three egg doses. Significant perivascular fibrosis was also observed in autopsy specimens from patients who died of this condition.
Conclusions: Repeatedly exposing mice to schistosomiasis causes a persistent PH phenotype, accompanied by perivascular fibrosis. Perivascular fibrosis may contribute to the persistent schistosomiasis-PH observed in humans with this disease.

Introduction

Pulmonary hypertension (PH) is characterized by vascular remodeling, right ventricular (RV) hypertrophy, and perivascular fibrosis. Many pulmonary vascular diseases develop after prolonged or repeated exposures, such as after many years of autoimmune disease, or with repeated hypoxia exposures in the setting of obstructive sleep apnea. Irreversibility of pulmonary pathology is a major challenge in PH, as the therapies currently available improve symptoms and slow progression but do not reverse established disease.

Dysregulated host inflammation probably contributes to the pathogenesis of many forms of PH, including that due to schistosomiasis, which due to its high prevalence is a common cause of PH worldwide. The *Schistosoma mansoni* parasite lays its eggs in the portal venous system of the host. The chronic and repeated infection causes pre-portal liver fibrosis, resulting in portal hypertension and the opening of portocaval shunts. These shunts enable the passage of eggs around the liver, from the portal system to the

Received: 26 September 2022
Revised: 23 March 2023
Accepted: 04 April 2023

Accepted Manuscript online: 04 April 2023
Version of Record published: 21 April 2023

Clinical Science (2023) **137** 617–631
https://doi.org/10.1042/CS20220642

systemic venous circulation, where the eggs embolize into the lungs. *Schistosoma* eggs have a diameter of ∼100 μm, lodging in pre-capillary vessels and resulting in significant localized Type 2 inflammation. This intrapulmonary inflammation is likely critical to the pathogenesis of vascular disease in *Schistosoma*-PH.

In mice experimentally exposed to *Schistosoma*, sensitization prior to intravenous egg challenge is required for the PH phenotype [1], indicating a requirement for adaptive immunity. Further, mice lacking B and T cells are protected from *Schistosoma*-PH [2]. Activating CD4 T cells in the lung to a Th2 phenotype results in significant localized expression of IL-4 and IL-13, and mice absent these cytokines globally or in CD4 T cells specifically are protected from *Schistosoma*-PH [2,3]. IL-4/IL-13 expression results in the recruitment of $CCR2^+$ monocytes to the adventitial space, where these cells express thrombospondin-1 (TSP-1), which functionally activates TGF-β causing vascular remodeling [4].

While inflammation is a clear driver of schistosomiasis-PH, it is unclear how host inflammation evolves and contributes to the persistence of the PH disease after the initial triggering event. Clinical data indicate that despite treatment with antihelminthics such as praziquantel, schistosomiasis PH in humans persists and progresses [5–7]. Furthermore, modern autopsy case series of individuals who died of *Schistosoma*-PH reveal substantial vascular remodeling but no significant egg antigens, consistent with parasite eradication but the progressive vascular disease [8].

Here, we explore the concept that the duration of disease and parasite exposure contribute to the development of persistent pulmonary pathology. We tested the specific hypothesis that repeated exposure to *Schistosoma* antigens contributes to the development of persistent PH, using a mouse model of repeated intravenous egg administration. Overall, we observed that repeated *Schistosoma* exposure leads to persistent PH accompanied by perivascular fibrosis, a pathologic feature we also found present in human lung tissue from individuals who died of *Schistosoma*-PH.

Methods

Animals

C57BL6/J mice were purchased from Jackson Laboratories (#00664, Bar Harbor, ME). Female mice were used between 6 and 8 weeks of age at the commencement of the experiment, as PH is more prevalent in females [9] and thus may be more representative of the human condition; we have not previously observed a difference in *Schistosoma*-PH phenotype between males and females; and we have found older male mice may develop spontaneous mild PH which would be confounding in the longer time course experiments. All animals were housed under specific pathogen-free conditions in an American Association for the Accreditation of Laboratory Animal Care-approved facility at the University of California, San Francisco (UCSF). All animal studies were approved by the UCSF Institutional Animal Care and Use Committee. The animal procedures followed were approved by institutional guidelines and conducted at UCSF.

Schistosoma-induced PH model

Schistosoma mansoni fresh and live eggs were obtained by homogenizing and purifying the livers of Swiss-Webster mice pre-infected with *S. mansoni* cercariae from the Biomedical Research Institute (Rockville, MD). Similar to prior publications [3,4,10], the experimental mice were intraperitoneally (IP) sensitized with 240 *S. mansoni* eggs/gram body weight, and then 2 weeks later intravenously (IV) challenged with 175 *S. mansoni* eggs/gram body weight, and right heart catheterization (RHC) was performed at +7 days (Group B; see Figure 1A), +14 days (Group C), +21 days (Group D), or +28 days (Group E) after the IV challenge. Control mice were unexposed to *S. mansoni* eggs (Group A1), only IP +14 days (Group A2) or only IP +28 days sensitized (Group A3). In the multiple IV challenge model, IP sensitized mice were IV challenged with three doses of *Schistosoma* at 2 weeks intervals for 3 total IV doses. RVSP was measured at +7 days (Group F; see Figure 2A) or +21 days (Group G) following the third IV challenge. The dose of IV eggs was the same 175 *S. mansoni* eggs/gram body weight each time.

PD-1 neutralizing antibody treatment

We administered neutralizing antibodies targeting PD-1 to selected mice, or isotype control antibodies to control animals. For PD-1 intervention, mice were injected with 200 μg of anti-PD-1 antibody (clone 29F.1A12, BioXcell) or rat IgG2a isotype control (clone 2A3, BioXcell), administered intraperitoneally with the regimens outlined in Supplementary Figure S10A, with the dose based on prior publications [11].

Assessment of PH

To measure hemodynamics, the mice underwent terminal RHC by an open chest method as described previously [3,4,10]. Briefly, the mice were sedated with intraperitoneal ketamine-xylazine injection, and a tracheostomy tube

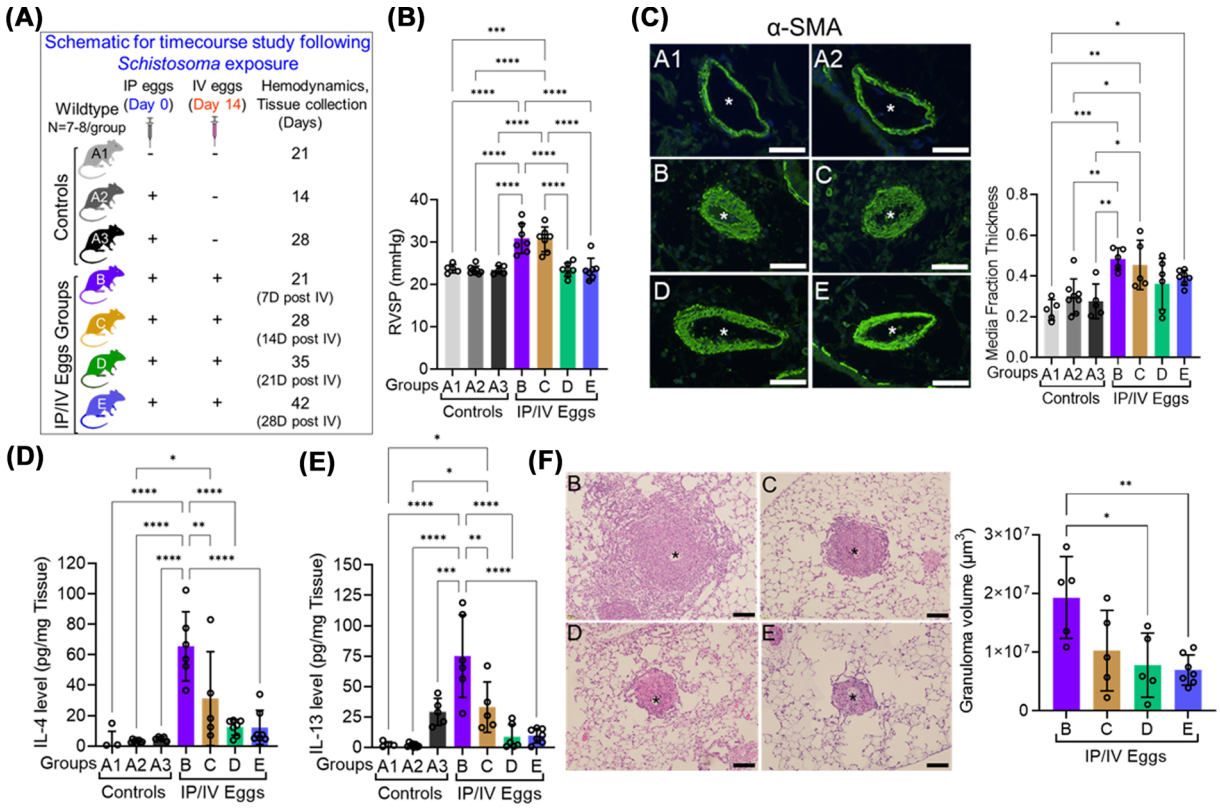

Figure 1. The timecourse following a single dose of *Schistosoma* challenge demonstrates inflammatory PH pathology which peaks and then substantially resolves at later timepoints

(**A**) Schematic showing *Schistosoma* exposed experimental groups that were analyzed at different timepoints. (**B**) Right ventricular systolic pressure (RVSP) by right heart catheterization (N = 5–8/group). (**C**) Qualitative and quantitative fractional thickness of the pulmonary vascular by morphometry (N = 5–8/group); *: vessel lumen; scale bars: 50 μm. (**D**) IL-4 and (**E**) IL-13 protein concentrations by ELISA (N = 5–8/group). (**F**) Peri-egg granuloma volumes as measured by stereology (N = 5–7/group); *: eggs at center of granuloma; scale bars: 100 μm. Group A1 (*Schistosoma* unexposed) and Group A2 (*Schistosoma* sensitized only) were controls. Groups B, C, D, and E were sensitized and challenged with *Schistosoma*, and analyzed at different timepoints. Mean ± SD plotted; analysis of variance (ANOVA) $P<0.0001$, $P<0.001$, $P<0.01$ for RVSP, media thickness and granuloma volume, respectively, whereas, $P<0.0001$ for both IL4 and IL13; post-hoc Tukey tests shown: *$P<0.05$, **$P<0.01$, ***$P<0.001$, ****$P<0.0001$. IP: intraperitoneal *Schistosoma* eggs; IV: intravenous *Schistosoma* eggs.

was placed, and mechanical ventilation was initiated at 6cc/kg. The abdomen and diaphragm were opened by careful dissection to avoid any blood loss, and a 1 Fr pressure–volume catheter (PVR-1035, Millar ADInstruments, Houston, TX) was placed directly into the right ventricle (RV), and then the left ventricle (LV) chambers through the free walls.

Protein quantification

Frozen lung tissues were macerated and sonicated in RIPA buffer (Thermo Scientific, Rockfield, IL, U.S.A., cat. # 89900) containing protease and phosphatase inhibitor cocktails (EMD Millipore, MA, U.S.A., cat. #s 539131 and 524625, respectively). Total protein concentration was determined by Bradford assay. IL-4, IL-13, and TGF-β1 levels were quantified in the whole lung lysates by ELISA using the commercial kits (Mouse IL-4 Quantikine ELISA Kit, M4000B; Mouse IL-13 Quantikine ELISA Kit, M1300CB and TGF-β1 Quantikine ELISA Kit, MB100B from R&D Systems, Inc. Minneapolis, MN; Mouse C3a ELISA Kit, MBS268280, MyBioSource, San Diego, CA). Active TGF-β1 was quantified using the lung lysates directly; total TGF-β1 was quantified by acid-treating the samples prior to quantification, per the manufacturer's directions, using the same kit.

Clinical Science (2023) **137** 617–631
https://doi.org/10.1042/CS20220642

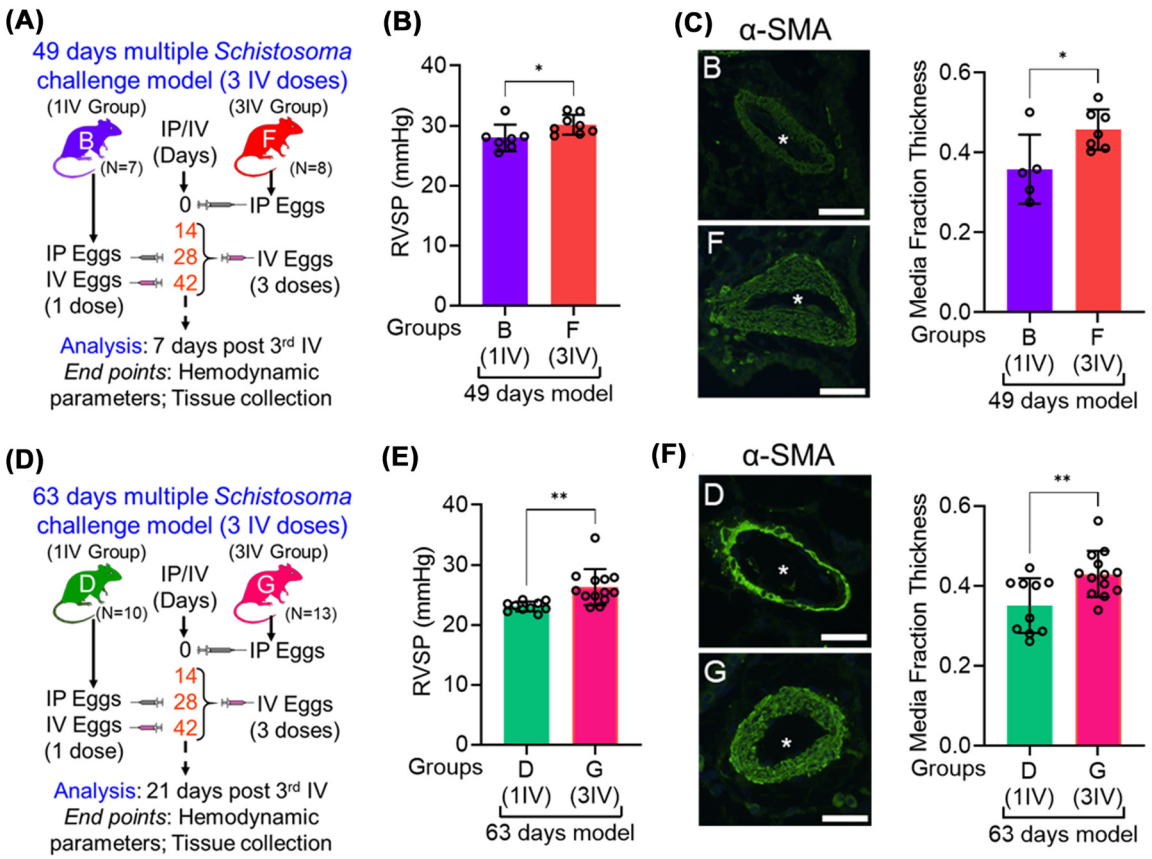

Figure 2. Repeated *Schistosoma* challenge in mice causes persistent PH at a late timepoint

(**A**) Schematic of the model of thrice challenged mice, analyzed 7 days after the final dose. (**B**) Right ventricular systolic pressure (RVSP); ($N = 7$–8/group). (**C**) Qualitative and quantitative fractional thickness of the pulmonary vasculature ($N = 5$–7/group); *: vessel lumen; scale bar: 50 μm. (**D**) Schematic of the model of thrice challenged mice, analyzed 21 days after the final dose. (**E**) RVSP ($N =$ 10–13/group). (**F**) Qualitative and quantitative pulmonary vascular fractional thickness ($N = 10$–13/group); *: vessel lumen; scale bar : 50 μm. Mean ± SD plotted; *t* tests shown; $^*P<0.05$, $^{**}P<0.01$. IP: intraperitoneal *Schistosoma* eggs; IV: intravenous *Schistosoma* eggs.

Mouse cytokine array analysis

A mouse cytokine array was performed on lung tissue lysates per the manufacturer's guidelines (Proteome ProfilerTM Array, R&D System, MN, U.S.A.). In brief, 200 μg protein from whole lung lysates was mixed with binding buffer and incubated overnight with a membrane containing 40 antibodies for inflammatory markers. Chemiluminescent imaging of protein blots using a BioSpectrum™ 510 Imaging System integrated with a VisionWorksLS image capture and analysis software package (Ultra-Violet Products, LLC, Upland, CA) were used to capture the images and perform quantification.

RNA quantification

Real-time polymerase chain reaction (RT-PCR) was used to quantify the expression of mRNA transcripts in lung lysates using the primers in Supplementary Table S1. iScript cDNA Synthesis kit (Bio-Rad Laboratories, Hercules, CA, U.S.A., cat.#: 1708891) was used for first-strand cDNA synthesis using 1 μg RNA. RT-PCR was performed in duplicate for each gene and each sample. TaqMan™ Gene Expression Master Mix (Applied Biosystems, cat.#: 4369016) was used to see the expression of target genes using StepOnePlus™ Real-Time PCR System (Applied Biosystems) using the following conditions: Holding stage: 55°C for 10 min, 95°C for 3 min; Cycling stage: 95°C, 5 s and 60°C, 10 s; no. of cycles = 40. A reaction volume of 20 μl was used. To calculate relative transcript quantities, the $2^{-\Delta Ct}$ method was used with β-actin as the endogenous reference genes. In addition, *Col1a1* mRNA had been previously quantified

using a HiSeq 2000 RNA sequencing (RNA-seq) system (Illumina, San Diego, CA); data are deposited in National Center for Biotechnology Information's GEO dataset GSE49116 [12].

Vascular remodeling and granuloma assessment

Immunostaining for α-smooth muscle actin was performed on FFPE mouse lung tissue using the reagents listed in Supplementary Table S2. To quantify fractional media thickness, images of 10–12 vessels of each specimen from the α-smooth muscle actin-stained slides were acquired using a Nikon Eclipse 80i microscope (Nikon, Melville, NY) with an Olympus DP74 color camera (Olympus, Waltham, MA). The external and internal perimeters of the media were identified using image processing software (ImagePro v10, Media Cybernetics, Bethesda, MD), the radii of each layer calculated ($r = \text{sqrt}[A/\pi]$), and the fractional thickness calculated from the difference between the two radii divided by the external radius. Peri-egg granuloma volumes were measured using the optical rotator stereological method, with hematoxylin and eosin stained FFPE tissue, using 8–10 images of granulomas with a single visible egg acquired for each sample, and the rotator method for object volume estimation applied using the egg as the central point (ImagePro) [3,13].

Localization of signaling molecules, cells, and fibrosis assessment

Immunostaining for pSmad2/3, collagen-producing cells such as fibroblasts, and macrophages was performed on FFPE mouse lung tissue using the reagents listed in Supplementary Table S2. Collagen-producing cell density quantification as performed as the ratio of $HSP47^+$ cells in the adventitial space, or the intima plus media space, divided by the area analyzed, using Stepanizer v1.8 (stepanizer.com), and macrophage density using $CD68^+$ cells in the same manner. Picrosirius red staining was used to quantify perivascular fibrosis in unexposed and IP/IV egg-exposed mice, using standard protocols [14]. Ten images of each mouse were acquired at 10× magnification and superimposed on a 1700-point grid using ImagePro software. Adventitial regions of interest (ROI) were identified, and points intersecting with collagen (positive picrosirius red polarization) were counted, as compared with all points falling within the ROI, and used to determine the volume fraction of vascular fibrosis (ImagePro).

Combined RNA *in situ* hybridization and immunofluorescence staining

Mice were killed in CO_2 and then dissected to expose the thoracic cavity. The right ventricle was perfused with PBS. Lungs were inflated using 2% low melting point agarose at 37degC. After inflation, lungs were fixed in 10% neutral buffered formalin for 24 h, then transferred to 70% ethanol in water. After 48 h, the lungs were paraffin embedded and cut into 5 μm sections. The RNA Scope [15] Multiplex Fluorescent V2 Assay (ACD Bio, Newark CA, #323136) protocol for formalin-fixed paraffin-embedded tissue was followed as per the manufacturer's directions. Hybridization probes for Col1a1 (Mm-Cola1a1-C2, #319371-C2) and Tgfb1 (Mm-Tgfb1-C1, #407751) were used. Probes were imaged using the following Opal fluorophore dyes (Akoya Biosciences, Marlborough, MA): Opal 570 (FP1488001KT) for Tgfb1 and Opal 620 (1495001KT) for Col1a1, respectively. After completing the RNA scope protocol, slides were washed in phosphate buffered saline (PBS) and then immediately stained overnight with pre-conjugated Acta2-Alexa488 antibody (Clone 1A4, Invitrogen 53-9760-82) at a 1:200 dilution along with Alexa 750 conjugated hydrazide (Abnova U0261) at a 1:400 dilution in a buffer containing 5% goat serum and 1% bovine serum albumin in PBS. Slides were washed in PBS containing 0.5% Tween-20, stained with DAPI at a 1:500 dilution in PBS, and then mounted in Prolong Gold (Invitrogen P36930). Sections were imaged on a Leica Sp8 inverted confocal microscope with a white light laser system using a 20× glycerol immersion objective. Z-stacks (1 μm sections) at 1024 × 1024 resolution were taken of all observable blood vessels. Images were processed using ImageJ [16], with published images representing a maximal intensity projection of the two best z-stack slices.

Human tissue fibrosis assessment

Picrosirius red staining [14] and immunostaining (using the reagents listed in Supplementary Table S3) of human lung tissue was performed on FFPE samples of two types of human lung tissue: (1) *Schistosoma*-PH, obtained at autopsy from patients who died of schistosomiasis-associated PH in Recife, Brazil; and (2) control explanted lung tissue, from unsuccessful lung donors collected by the Pulmonary Hypertension Breakthrough Initiative in the US. The UCSF IRB approved all human studies.

Statistics

Prism (v9, GraphPad, San Diego, CA) was used for statistical analyses and graphs. Differences between two groups were assessed by *t*-test; for ≥3 groups, differences were assessed by ANOVA followed by post-hoc Tukey test.

Clinical Science (2023) **137** 617–631
https://doi.org/10.1042/CS20220642

Non-normally distributed data or groups with samples <5 were analyzed by non-parametric analysis. *P* values less than 0.05 were considered statistically significant.

Results

A single *Schistosoma* intravenous challenge leads to Th2 inflammation and PH, which largely resolves after 14 days

To understand the long-term impact of *Schistosoma* exposure on PH phenotypes, we performed a time course analysis of a well-established experimental mouse model of *Schistosoma* PH, which uses intraperitoneal (IP) egg sensitization followed by intravenous (IV) egg challenge [4,10], by analyzing groups of mice at different times following the IV egg challenge (Figure 1A). Compared with either totally unexposed mice (Group A1), sensitized but unchallenged mice at either 14 days (*Group A2*) or 28 days (*Group A3*) did not develop a PH phenotype. Following IV challenge, we observed significantly higher right ventricle systolic pressure (RVSP), medial remodeling, and right ventricle (RV) hypertrophy in sensitized mice that were challenged with a single intravenous (IV) dose of *Schistosoma* eggs at +7 days after the IV eggs were given (Group B; Figure 1B,C and Supplementary Figure S1A), particularly in comparison to the unexposed mice (Group A1), but also in contrast with the IP challenged mice (Groups A2 and A3). These phenotypes were maintained through +14 days after the intravenous *Schistosoma* challenge (Group C). Thereafter, the pathologic phenotype substantially, but not entirely, resolved at days +21 and +28 after intravenous *Schistosoma* exposure (Groups D and E, respectively). Even at +28 days, there remained a modest increase in medial thickness and RV hypertrophy compared with the unchallenged mice.

We then investigated the timecourse of Th2 inflammation. We observed maximal IL-4 and IL-13 cytokine levels, and peri-egg granuloma volumes, at the +7 day timepoint after the *Schistosoma* IV challenge, which progressively declined over the next 21 days (Figure 1D–F). By day +28, the cytokine levels had returned to approximately baseline values. These data are consistent with the concept that host inflammation leads to vascular remodeling, and that resolution of inflammation begins prior to the resolution of vascular remodeling.

We did not observe any difference in left ventricular pressures, heart rate or animal body weight in the *Schistosoma* exposed mice analyzed at the various timepoints (Supplementary Figure S1B–E). Because the mice exposed to IP eggs alone (Group A2) had essentially the same phenotype as unexposed mice (Group A1), we used unexposed mice for the control mice for the remainder of our experiments.

Repeated *Schistosoma* exposure leads to persistent PH

To investigate the impact of repeated exposure to *Schistosoma*, and to better model the repeated and chronic infection in humans, we challenged previously sensitized mice with three consecutive doses of IV *Schistosoma* eggs every 2 weeks, as compared with mice that were sensitized and then challenged with a single dose of *Schistosoma*. We observed at +7 days after the last IV egg challenge, the group that received 3 IV doses (i.e., Group F, Figure 2A) had a higher RVSP and greater vascular remodeling as compared with the group that had received just 1 IV dose (as in Group B above; Figure 2B,C). There was no difference in RV hypertrophy (Supplementary Figure S2A). Overall, these data indicate the degree of peak PH severity was mildly greater after multiple *Schistosoma* exposures.

We then investigated whether the PH pathology resolved in the chronically challenged mice, studying the +21 day timepoint after the final IV egg dose in mice that received 3 IV egg challenges (termed Group G, Figure 2D). A comparison was made to the same timepoint in mice challenged just once, as the PH phenotype had largely resolved by this time in the mice that received a single IV egg dose (i.e., Group D in Figure 1B). We found the increased RVSP and media remodeling now persisted in mice challenged with three doses (Figure 2E,F, and Supplementary Figure S2B and C).

We did not observe any difference in left ventricular pressures, heart rate, or animal body weights between the single versus thrice challenged mice at either the +7 or +21 day timepoint (Supplementary Figure S3).

Persistent *Schistosoma*-PH is accompanied by vascular fibrosis in repeatedly challenged mice

We then explored potential mechanisms underlying the persistent PH phenotype observed in the thrice IV challenged as compared with the single IV challenged mice, interrogating for differences in the pulmonary vasculature that might have been induced by the Th2 inflammation and TGF-β signaling that occurs in *Schistosoma*-PH [10,17,18]. Clinical and experimental pulmonary fibrosis can be complicated by PH [19,20], and peri-vascular fibrosis is a pathological feature of PH [21]. Thus, fibrosis of the pulmonary vasculature is a plausible contributor to the persistent PH observed after multiple *Schistosoma* exposures.

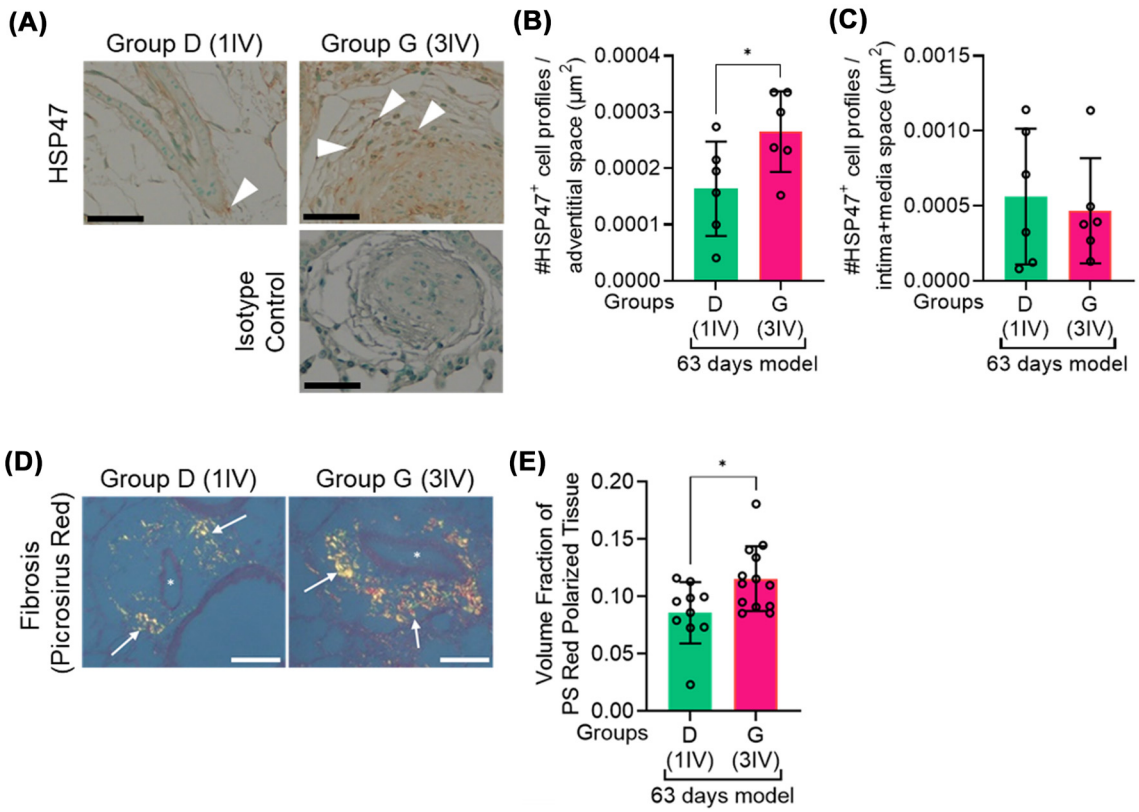

Figure 3. Increased HSP47⁺ collagen-producing cells and peri-vascular collagen are present in mice that received multiple *Schistosoma* challenges

(**A**) HSP47 stain of Groups D and G, and an isotype control. Arrowheads mark HSP47-positive cells; scale bars: 50 μm. Density of HSP47-positive cells in the (**B**) perivascular/adventitial and (**C**) intima and media combined (within the adventitia) spaces ($N = 6$/group). (**D**) Picrosirus red stain of Groups D and G. Arrows mark representative areas of high collagen protein deposition; *: vascular lumen; scale bars: 100 μm. (**E**) Volume fraction of polarized tissue in the perivascular space ($N = 10$–13/group). Mean ± SD plotted; *t-test $P<0.05$; IV: intravenous *Schistosoma* eggs.

We analyzed the density of collagen-producing cells, such as fibroblasts by immunostaining around and within the remodeled vessels, using an anti-HSP47 antibody; HSP-47 is a chaperone protein required for collagen protein synthesis [22]. We found a significant increase in the number of collagen-producing cells in the adventitial space, around the vessels, in the thrice challenged mice compared with the singly challenged mice analyzed 21 days after the final egg dose (e.g., Group D vs. Group G; Figure 3A,B). We did not find a difference in the density of collagen-producing cells within the combined media and intima compartments of the pulmonary vasculature (Figure 3C).

To determine if there was a potential functional difference in extracellular matrix deposition resulting from a greater number of collagen-producing cells, we studied the perivascular collagen protein density using picrosirius staining, analyzed using cross-polarization, which provides spatial quantification of Type 1 collagen specifically [14]. We observed that the collagen content in the perivascular space of the thrice challenged mice was significantly greater than in those challenged just once (Figure 3D,E). Significant fibrosis was not observed in the combined media and intima compartments. Following a single *Schistosoma* egg challenge, we observed no difference in the perivascular collagen deposition analyzed at different timepoints (Supplementary Figure S4).

Pulmonary fibrosis can be triggered by Th2 inflammation and TGF-β [23,24]. To assess the possible Th2-regulation of collagen in the *Schistosoma*-PH model, we analyzed a previously published whole lung mRNA dataset from our group (GSE49116), which revealed an increase in *Col1a1* expression in sensitized and singly IV challenged mice, at a timepoint 7 days after the IV eggs were administered, as compared to unexposed mice (equivalent of Groups A1 and B; Supplementary Figure S5). The increased *Col1a1* observed in *Schistosoma*-exposed wild-type mice in this dataset

Clinical Science (2023) **137** 617–631
https://doi.org/10.1042/CS20220642

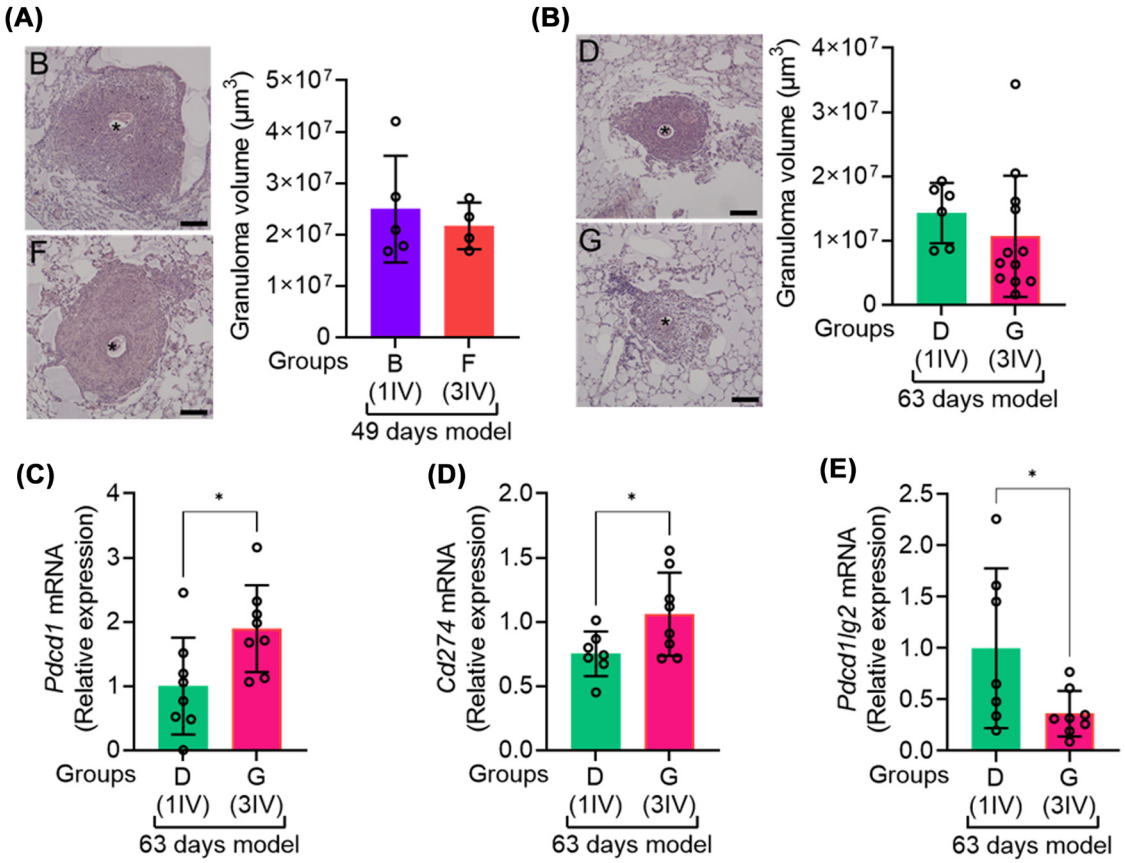

Figure 4. Granuloma volumes are not significantly different in mice that received multiple *Schistosoma* challenges, while T-cell exhaustion markers increase

(**A**) Peri-egg granuloma volumes ($N = 4$–5/group) in Groups B and F; *: eggs at center of granuloma; scale bars: 100 μm. (**B**) Peri-egg granuloma volumes in Groups D and G ($N = 6$–11/group); *: eggs at center of granuloma; scale bars: 100 μm. Whole-lung mRNA expression quantified by RT-PCR of (**C**) *Pdcd1* (PD1), (**D**) *Cd274* (PDL1) and (**E**) *Pdcd1lg2* (PDL2) in *Schistosoma* exposed-mice analyzed after 21 days of last *Schistosoma* challenge ($2^{-\Delta Ct}$ method; relative to β-actin housekeeping gene; $N = 7$–8/group). Mean ± SD plotted; *t* tests shown: $^*P<0.05$. IV: intravenous *Schistosoma* eggs.

was suppressed in *Schistosoma*-exposed $Il4^{-/-}Il13^{-/-}$ mice, which have blocked Th2 inflammation, implicating Th2 inflammation as a potential driver of the vascular fibrosis in *Schistosoma*-PH.

The Th2 inflammation and TGF-β signaling is largely resolved after repeated IV egg challenge

Having identified a difference in vascular fibrosis in the repetitively challenged mice after 21 d, we next sought to characterize the degree of inflammation at the same timepoint. We first looked at the +7 day timepoint after the final dose of IV eggs (Group B versus Group F), at a time of peak pathology. We found that the estimated peri-egg granuloma volumes, as a readout of overall inflammation, were not different between the two groups (Figure 4A and Supplementary Figure S2D), nor were there differences in IL-4 and IL-13 in whole lung lysates as measured by ELISA (Supplementary Figure S2E and F, and Supplementary Figure S6A and B). We then analyzed the thrice and singly challenged mice 21 days after the final egg dose (Groups D and G). Again, we found no difference in peri-egg granuloma volume (Figure 4B and Supplementary Figure S2D), nor a difference in IL-4 or IL-13 concentrations between the two groups (Supplementary Figure S2E and F, and Supplementary Figure S6C and D).

Suspecting that repeated exposure to the same antigen could induce fatigue of the immune system, we interrogated the expression of the T cell inhibitory receptor PD1 and its ligands PDL1 and 2 by RT-PCR of lung lysates. We found

increased expression of PD1 (expressed by Pdcd1) and PDL1 (Cd274), but lower expression of PDL2 (Pdcd1lg2) (Figure 4C–E). Overall, this is consistent with a phenotype of T-cell exhaustion in the repetitively challenged mice.

We also looked for changes in T-cell phenotype or complement as potential mechanisms underlying the persistent PH by analyzing mRNA expression. We found no differences in *Foxp3*, *Il17a*, or *Il17f* between the two groups suggesting unchanged Th17 and Treg CD4 T cells (Supplementary Figure S7A–C). We also found no change in the mRNA expression of complement members *C3, C5*, or *C1q* or protein level of C3a between the two groups (Supplementary Figure S7D–G).

Acutely, Th2 inflammation triggers TGF-β activation to cause *Schistosoma*-PH [4], but with quelling of the Th2 inflammation it could be that TGF-β signaling could also be now suppressed. We found no differences in active or total TGF-β protein or the mRNA expression of prototypical TGF-β targets *Pai1* or *Smad7* in whole lung lysates, or phospho-Smad2/3 protein by immunostaining (*Group D vs*. Group G, Supplementary Figure S8).

We sought to identify additional inflammatory proteins which could be different between the singly and thrice challenged mice at this late timepoint by using a protein array for mouse cytokines on the lung lysates. Seven additional proteins were consistently seen in all samples (Supplementary Figure S9A): CXCL12, CCL5, IL-1Ra, IL-16, sICAM-1, TIMP-1, and C5/C5a. However, none of these proteins differed between the two groups (Supplementary Figure S9B).

We also sought to identify if there might be a difference in macrophage density between the singly and thrice challenge mice at the 21 day timepoint by immunostaining for CD68. We did not observe any difference in macrophage density in either the adventitial space or the intima plus media space (Supplementary Figure S10).

Together, these data suggest that while Th2 inflammation and TGF-β signaling are critical to early disease pathogenesis in *Schistosoma*-PH, these drivers may no longer be necessary for the persistent PH accompanied by vascular fibrosis observed at later timepoints.

Hypothesizing that PD-1/PD-L1 signaling causing T-cell exhaustion may impact the persistent PH phenotype, we attempted to target PD-1 using a neutralizing antibody approach. However, this treatment did not modify the persistent PH phenotype (Supplementary Figure S11).

In situ RNA hybridization also suggests vascular fibrosis develops in repeatedly challenged mice

To additionally validate the observation of increased peri-vascular fibrosis, we used *in situ* RNA hybridization (RNAScope). We began with probing tissue from single IV challenged mice at the +7 day timepoint, as compared with unexposed mice (Group A1 and Group B). We observed that the *Schistosoma*-challenged mice had evidence of increased TGF-β1 mRNA expression, consistent with the known mechanism of Th2-driven inflammation causing TGF-β signaling [4], as well as increased expression of Col1a1 mRNA (Figure 5A).

We then probed the thrice IV challenged versus single IV challenged mice, both at 21 d after the final IV eggs were given (Group D and Group G). We observed that the expression of Col1a1 mRNA was prominent in the pulmonary vascular compartment in both groups, but was particularly more prominent in the perivascular space in the thrice challenged mice (Figure 5B,C). The expression of TGF-β1 appeared similar in the two groups, corroborating the absence of a difference in TGF-β signaling observed above.

Human *Schistosoma*-PH is also characterized by vascular fibrosis

To determine if the perivascular fibrosis we observed in multiply challenged mice may also be relevant to the chronic disease in human *Schistosoma*-PH, we analyzed perivascular fibrosis in four lung specimens collected at autopsy from patients that died of this condition in Brazil, also using picrosirius red staining. We observed that 2 of the 4 specimens had substantial perivascular fibrosis, particularly around pulmonary vascular lesions and in the vicinity of schistosomal pigment (which is frequently observed near pulmonary vascular lesions [25]), and to a much greater extent than was observed in three control specimens (Figure 6). Demographic data were unavailable for the four *Schistosoma*-PH specimens; brief demographic data for the three control specimens are listed in Supplementary Table S4.

We also interrogated for a potential change in fibroblast density in human *Schistosoma*-PH by immunostaining for vimentin, a marker of mesenchymal cells including fibroblasts. As compared with control human tissue (Supplementary Figures S12A–C), we observed an apparent increase in mesenchymal cell density, particularly in the media vascular compartment in *Schistosoma*-PH specimens (Supplementary Figures S12D–E). We also observed significant vimentin staining in plexiform lesions in the *Schistosoma-PH* tissue (Supplementary Figure S12F), as previously reported in idiopathic PH [26].

Clinical Science (2023) **137** 617–631
https://doi.org/10.1042/CS20220642

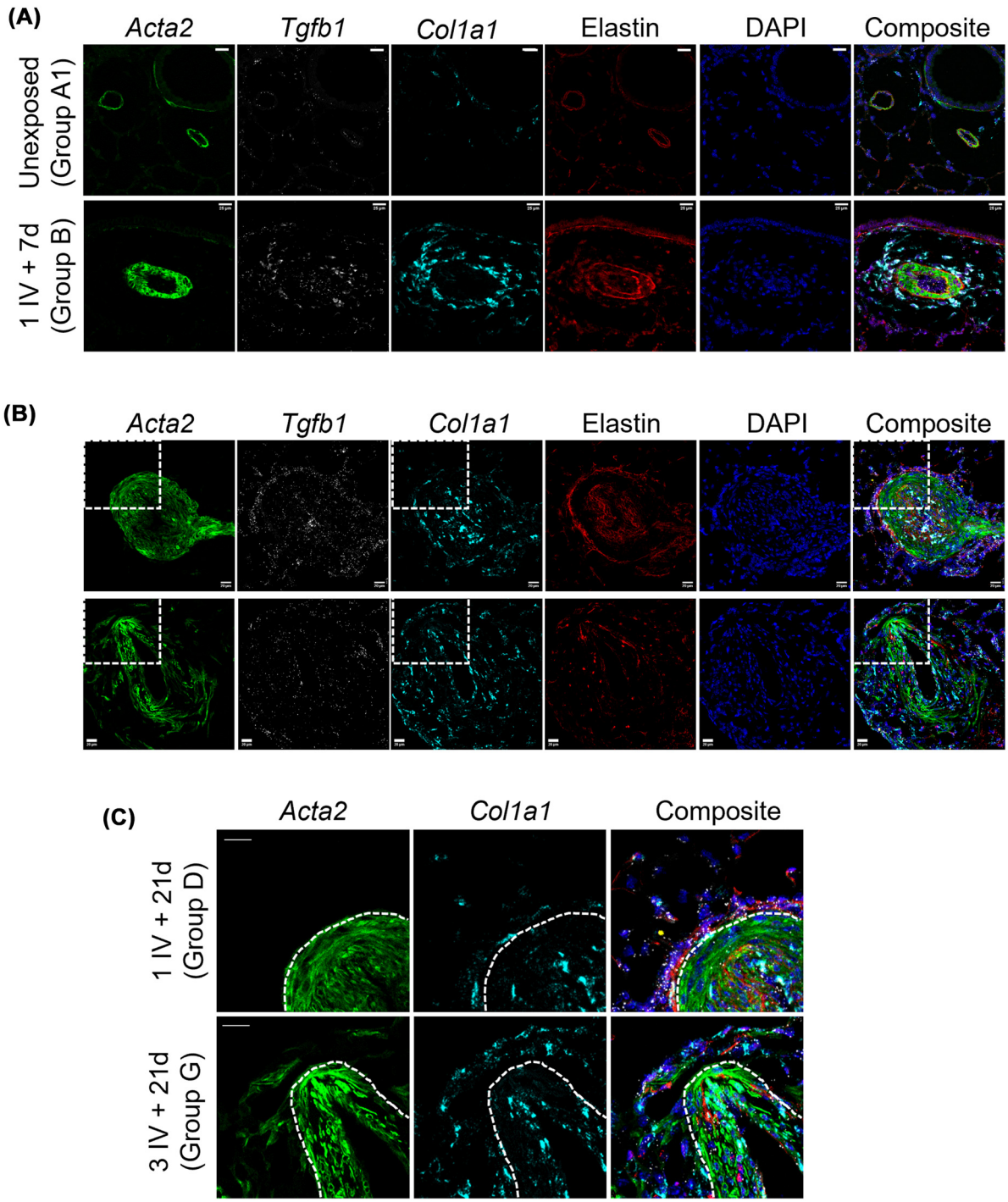

Figure 5. ***In situ*** **RNA hybridization suggests increased collagen in the adventitial space in repetitively** ***Schistosoma*****-challenged mice**

(**A**) RNA probes for Tgfb1 (white; TGF-β1) and Col1a1 (cyan; Collagen 1A1 protein), with immunostaining for Acta2 (green; expresses β-actin protein), hydrazide staining for elastin (red), and DAPI staining for nuclei (blue); and composite images of all channels shown, for control or single IV challenged mice at +7 days (Group A1 and Group B respectively, per Figure 1A). Representative pulmonary vessels from $N = 1$ Group A1 and 2 Group B mice/group. Scale bars: 25 μm. (**B**) RNA probes for the same transcripts and structural components as in (**A**). Representative pulmonary vessels from $N = 2$ mice/group; scale bars: 20 μm. Dotted lines show the inset in panel (C). (**C**) Magnified view of vessels in panel (B), showing the distribution of Col1a1 outside the exterior edge of the medial compartment, versus inside the exterior edge of the medial compartment; scale bars: 20 μm. Dotted lines demarcate the exterior edge of the medial compartment; L: lumen; M: media.

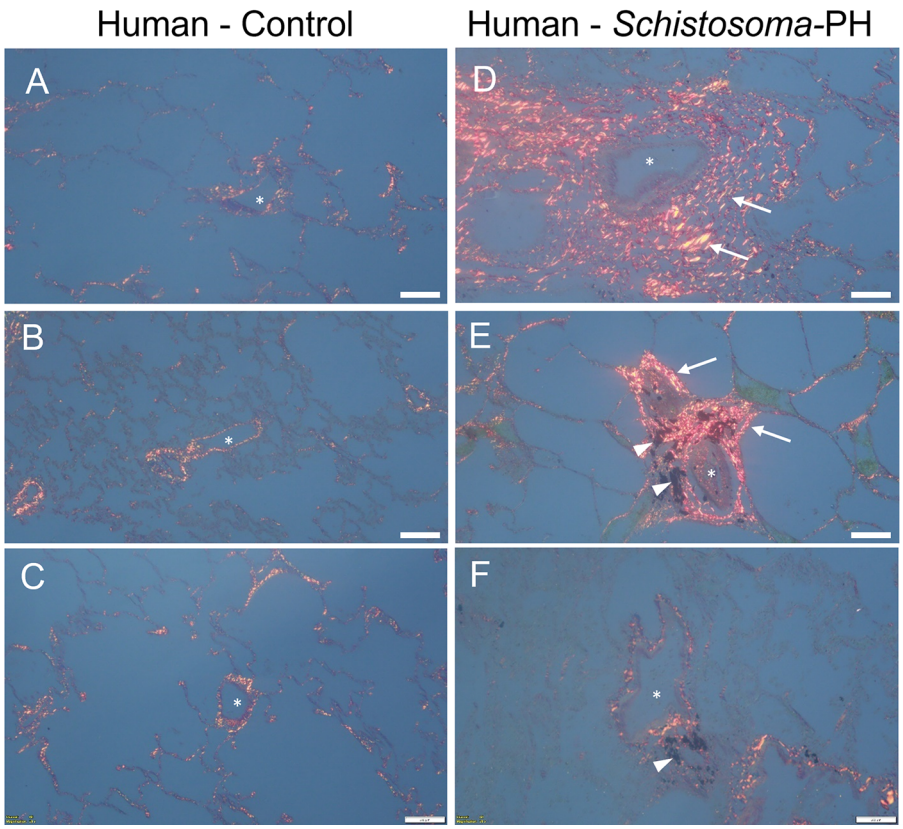

Figure 6. Evidence of perivascular fibrosis around remodeled lung vessels from autopsy cases of patients who died of schistosomiasis-associated PH, as compared to control lung tissue

(**A–C**) Representative images of picrosirus red stained lung tissue from three lung donors. (**D,E**) Two of four cases of *Schistosoma*-PH analyzed demonstrated substantial perivascular lung fibrosis. The vessels here have substantially increased thickness of the vessel wall, consistent with the pathology of pulmonary arterial hypertension. (**F**) Representative image from 2 cases of *Schistosoma*-PH which did not have increased perivascular lung fibrosis. *: vessel lumen. Arrows: representative positive picrosirus red staining. Arrowheads: schistosomal pigment, which is often observed adjacent to vascular lesions in human *Schistosoma*-PH; scale bars: 100 μm.

Discussion

Here, we observed that a single exposure to intravenous *Schistosoma* eggs in sensitized mice induces a PH phenotype that is substantially self-resolving. In contrast, repeated exposures cause a persistent PH phenotype (Figure 7). This result suggests a progression to persistent disease as is observed in humans with chronic and repeated *Schistosoma* exposure as occurs in endemic settings. We observed the persistent disease correlated with the emergence of increased density of perivascular fibroblasts and fibrosis, even at a timepoint when the inflammation was largely resolved. Perivascular fibrosis is a pathologic feature that we also found in lung specimens from humans who died of this condition, although not universally so.

These data help interpret a discrepancy previously observed between the murine *Schistosoma*-PH model and human *Schistosoma*-PH, namely the treatment effect of antihelminthics such as praziquantel. Mice experimentally exposed to *Schistosoma* can model aspects of the human disease, but there are key limitations, including the absence of any schistosomal liver disease, and a relatively short time course. In mice infected with *Schistosoma* for a relatively short duration, praziquantel causes reversal of the PH phenotype [27]. In mice, it has been observed that the severity of the lung remodeling depends upon the duration and the number of eggs deposited into the lungs [28,29]. In contrast, in humans chronically infected with *Schistosoma*, the PH phenotype is not significantly altered with praziquantel treatment [5–7]. We suspect the timing is important: in humans, the PH condition develops after years or even decades of chronic infection [30], whereas mice develop *Schistosoma*-induced PH in weeks to months [1,28]. It should be

Clinical Science (2023) **137** 617–631
https://doi.org/10.1042/CS20220642

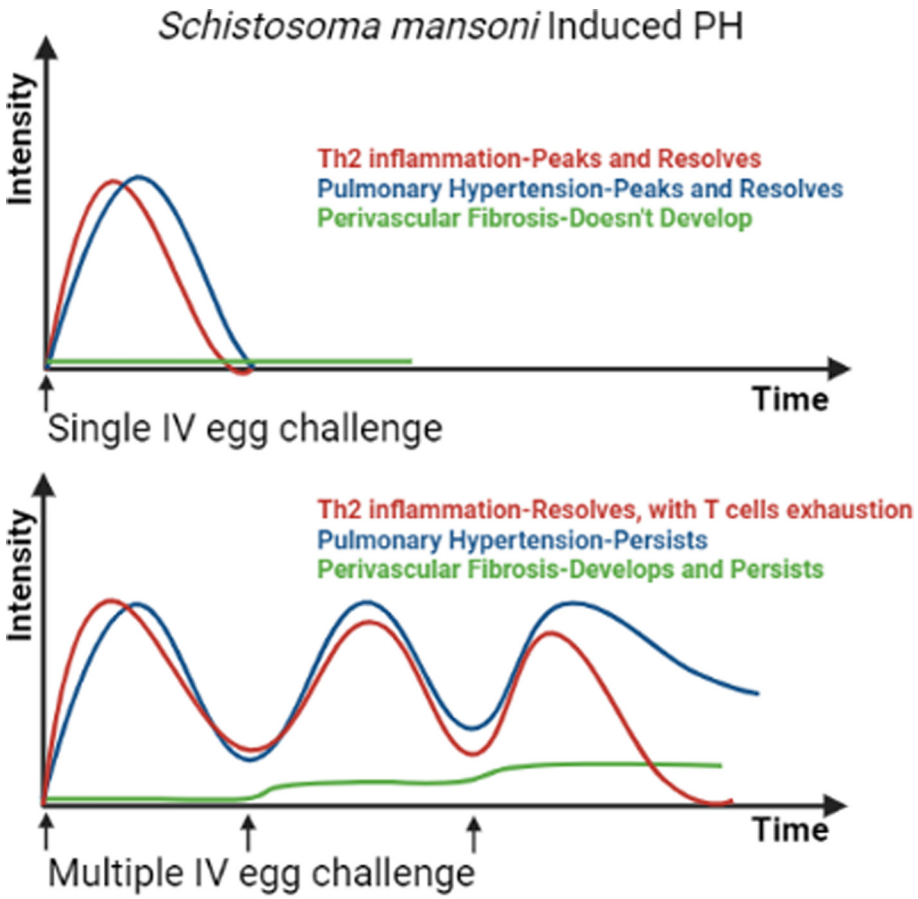

Figure 7. Outline of proposed changes in Th2 inflammation, fibrosis and PH phenotype following multiple IV *Schistosoma* egg challenges, as compared to a single IV egg challenge

In the single IV egg challenge model, the Th2 inflammation peaks and resolves; the PH phenotype peaks a little after the Th2 inflammation, and then resolves, and perivascular fibrosis does not develop. In the multiple IV egg challenged model, with each challenge episode the Th2 inflammation peaks and then partially resolves; with each challenge the PH phenotype increases in peak severity and resolves less; and perivascular fibrosis progressively increases and persists over time. Created with BioRender.com.

emphasized that diagnosing and treating schistosomiasis is still important in patients with *Schistosoma*-PH, as eradicating the parasite may slow the rate of PH progression, and likely helps reverse *Schistosoma*-induced fibrosis in the liver [31].

Schistosoma egg deposition can lead to tissue fibrosis [32]. Adventitial fibrosis has been observed in other clinical forms and experimental models of PH [33–35], and thus appears to be shared vascular pathology that fundamentally contributes to PH pathobiology. In particular, the adventitial fibroblast has been found to contribute to pulmonary vascular pathology through the secretion of extracellular matrix and cytokines that cause activation of other vascular cells [34]. We observed an increase in the density of collagen-producing cells around the vessels, likely but not definitively fibroblasts, as marked by HSP47 protein and Col1a1 mRNA expression. Increased stiffness of the pulmonary vasculature is clinically observed, along with increased pulmonary vascular resistance as a sign of vascular remodeling in PH [36]. PH can also be a complication of parenchymal lung fibrotic diseases, such as idiopathic pulmonary fibrosis [20], and experimental lung fibrosis can cause PH in animal models [37–39].

As a strong driver of Th2 inflammation, schistosomiasis infection has been observed to result in fibrosis around deposited eggs in the liver, which is dependent on IL-13 but independent of TGF-β [40]. In contrast, we have previously found the pulmonary vascular phenotype to be dependent on both IL-4/IL-13 and TGF-β [3,4]. We observed that collagen transcript expression is regulated in an IL-4/IL-13-dependent manner, as was described in the liver.

We observed an increase in whole lung PD1/PDL1 expression, suggestive of T cell exhaustion, a phenotype reasonably expected to occur following repeated antigenic challenges. As we have previously found CD4 Th2 T cells to

be critical to the pathogenesis of *Schistosoma*-PH, we wondered if T cells may be involved in the resolution of *Schistosoma*-PH, a role that could be impaired by an exhausted phenotype. However, blocking PDL1 by administering a neutralizing antibody did not modify the persistent PH phenotype, suggesting that T-cell exhaustion while present may not directly contribute to PH persistence or resolution after repeated challenges.

We have previously observed evidence of persistently increased IL-4 and IL-13 in Schistosoma-PH human autopsy tissue, including increased IL-13, IL-4Rα, and phosphorylated STAT6. However, other Type 2 inflammation receptors and cytokines were unchanged, including IL-13Rα1, IL-13Rα2, IL-4, and RELM-α [3,4,10]. Additionally, the plasma concentration of IL-13 was not elevated in subjects with Schistosoma-PH [41]. We also observed increased TSP-1 and TGF-β signaling in Schistosoma-PH autopsy tissue [3,4,10], and patients with *Schistosoma*-PH have increased TGF-β in their peripheral blood [41]. Overall, this suggests Type 2 inflammation and TGF-beta signaling may persist in human subjects with *Schistosoma*-PH, which is not fully recapitulated in the mouse model we are using. Furthermore, there may be other immune pathways now activated that are autonomously contributing to a persistent vascular remodeling phenotype.

There are several limitations of the present work. We do not have primary demographic data of the *Schistosoma*-PH human specimens, making it unclear how comparable they are to the control specimens. It remains unclear whether perivascular fibrosis is truly causal of the persistent PH or an epiphenomenon. To test this mechanistically, the role of fibrosis could be tested using antifibrotic small molecule inhibitors, or interrogating candidate drivers of fibrosis such as IL-4/IL-13 signaling, such as by deletion of STAT6 in fibroblasts specifically. It is also possible that the murine PH phenotype could resolve at later timepoints, although if so, it is likely that adding additional intravenous challenges to further approximate the human condition of chronic and recurrent exposure would result in a progressively more persistent phenotype.

In conclusion, we observed that repeated *Schistosoma* exposure leads to a persistent PH phenotype associated with perivascular fibrosis. The development of perivascular fibrosis may contribute to the persistent nature of *Schistosoma*-PH in some humans with this disease.

Clinical perspectives

- Schistosomiasis is a common cause of pulmonary hypertension worldwide, but why the disease persists despite antihelminthic therapy is unknown.
- We found that exposing mice to schistosomiasis causes pulmonary hypertension, which became persistent after repeated exposures, and was associated with the development of fibrosis around the lung blood vessels.
- We also observed perivascular fibrosis in human lung tissue from individuals that died of this condition.
- These results indicate that repeated schistosomiasis exposure can contribute to the development of persistent pulmonary hypertension, which may benefit from targeting the fibrosis that develops around the lung vasculature.

Data Availability

The data that support the findings of this study are available from the corresponding author upon reasonable request.

Competing Interests

The authors declare that there are no competing interests associated with the manuscript.

Funding

Grant funding was provided by American Heart Association [grant number 19CDA34730030]; ATS Foundation/Pulmonary Hypertension Association Research Fellowship; the Cardiovascular Medical Research Fund and United Therapeutics Jenesis Innovative Research Award (to R.K.); the UCSF Nina Ireland Program in Lung Health [grant number W81XWH2210457] from the US Department of Defense, and Fulbright Scholarship [grant number 12398-BR (to M.H.L.)]; and NIH [grant numbers R01HL135872

Clinical Science (2023) **137** 617–631
https://doi.org/10.1042/CS20220642

(to B.B.G.); P01HL152961 (to B.B.G. and R.M.T.); K08HL168310 (to M.H.L.); R01HL128734 and R01HL158868 (to E.S.); and R01HL135872-06S1 (to D.F.B.)].

Open Access

Open access for this article was enabled through a transformative open access agreement between Portland Press and the University of California.

CRediT Author Contribution

Rahul Kumar: Conceptualization, Data curation, Formal analysis, Funding acquisition, Investigation, Methodology, Writing—original draft. **Michael H. Lee:** Data curation, Formal analysis, Investigation. **Biruk Kassa:** Data curation, Investigation. **Dara C. Fonseca Balladares:** Data curation, Investigation. **Claudia Mickael:** Data curation, Investigation. **Linda Sanders:** Data curation. **Adam Andruska:** Data curation, Formal analysis. **Maya Kumar:** Data curation, Formal analysis. **Edda Spiekerkoetter:** Data curation, Formal analysis. **Angela Bandeira:** Data curation. **Kurt R. Stenmark:** Formal analysis. **Rubin M. Tuder:** Data curation. **Brian B Graham:** Conceptualization, Resources, Data curation, Formal analysis, Supervision, Funding acquisition, Investigation, Methodology, Writing—original draft.

Acknowledgements

Schistosome-infected mice were provided by the NIAID Schistosomiasis Resource Center at the Biomedical Research Institute (Rockville, MD) through NIH-NIAID Contract HHSN272201700014I for distribution through BEI Resources.

Abbreviations

CCR2, C-C chemokine receptor type 2; CD4, cluster of differentiation 4; IL-13, interleukin 13; IL4, interleukin 4; PD-1, programmed cell death protein 1; PDL2, programmed cell death ligand 2; PDL1, programmed death ligand 1; PH, pulmonary hypertension; RV, right ventricle; RVSP, right ventricular systolic pressure; TGF-β, transforming growth factor-β; Th2, T helper 2; TSP-1, thrombospondin-1.

References

1 Graham, B.B., Mentink-Kane, M.M., El-Haddad, H., Purnell, S., Zhang, L., Zaiman, A. et al. (2010) Schistosomiasis-induced experimental pulmonary hypertension: role of interleukin-13 signaling. *Am. J. Pathol.* **177**, 1549–1561, https://doi.org/10.2353/ajpath.2010.100063

2 Kumar, R., Mickael, C., Kassa, B., Sanders, L., Koyanagi, D., Hernandez-Saavedra, D. et al. (2019) Th2 CD4+ T cells are necessary and sufficient for schistosoma-pulmonary hypertension. *J. Am. Heart Assoc.* **8**, e013111, https://doi.org/10.1161/JAHA.119.013111

3 Kumar, R., Mickael, C., Chabon, J., Gebreab, L., Rutebemberwa, A., Rodriguez Garcia, A. et al. (2015) The causal role of IL-4 and IL-13 in schistosoma mansoni pulmonary hypertension. *Am. J. Respir. Crit. Care Med.* **192**, 998–1008, https://doi.org/10.1164/rccm.201410-1820OC

4 Kumar, R., Mickael, C., Kassa, B., Gebreab, L., Robinson, J.C., Koyanagi, D.E. et al. (2017) TGF-β activation by bone marrow-derived thrombospondin-1 causes Schistosoma- and hypoxia-induced pulmonary hypertension. *Nat. Commun.* **8**, 15494, https://doi.org/10.1038/ncomms15494

5 Fernandes, C.J.C.D.S., Jardim, C.V.P., Hovnanian, A., Hoette, S., Morinaga, L.K. and Souza, R. (2011) Schistosomiasis and pulmonary hypertension. *Expert Rev. Respir. Med.* **5**, 675–681, https://doi.org/10.1586/ers.11.58

6 Piscoya Roncal, C.G., Mendes, A.A., Muniz, M.T.C., de Oliveira, S.A., do Valle Neto, L.M., de Vasconcellos Piscoya, N.A. et al. (2019) Schistosomiasis-associated pulmonary arterial hypertension: survival in endemic area in Brazil. *Int. J. Cardiol. Heart Vasc.* **25**, 100373

7 Fernandes, C.J.C.S., Dias, B.A., Jardim, C.V.P., Hovnanian, A., Hoette, S., Morinaga, L.K. et al. (2012) The role of target therapies in schistosomiasis-associated pulmonary arterial hypertension. *Chest* **141**, 923–928, https://doi.org/10.1378/chest.11-0483

8 Graham, B.B., Chabon, J., Bandeira, A., Espinheira, L., Butrous, G. and Tuder, R.M. (2011) Significant intrapulmonary Schistosoma egg antigens are not present in schistosomiasis-associated pulmonary hypertension. *Pulm. Circ.* **1**, 456–461, https://doi.org/10.4103/2045-8932.93544

9 Umar, S., Rabinovitch, M. and Eghbali, M. (2012) Estrogen paradox in pulmonary hypertension: current controversies and future perspectives. *Am. J. Respir. Crit. Care Med.* **186**, 125–131, https://doi.org/10.1164/rccm.201201-0058PP

10 Graham, B.B., Chabon, J., Gebreab, L., Poole, J., Debella, E., Davis, L. et al. (2013) Transforming growth factor-β signaling promotes pulmonary hypertension caused by Schistosoma mansoni. *Circulation* **128**, 1354–1364, https://doi.org/10.1161/CIRCULATIONAHA.113.003072

11 Mall, C., Sckisel, G.D., Proia, D.A., Mirsoian, A., Grossenbacher, S.K., Pai, C.-C.S. et al. (2016) Repeated PD-1/PD-L1 monoclonal antibody administration induces fatal xenogeneic hypersensitivity reactions in a murine model of breast cancer. *Oncoimmunology* **5**, e1075114, https://doi.org/10.1080/2162402X.2015.1075114

12 Graham, B.B., Chabon, J., Kumar, R., Kolosionek, E., Gebreab, L., Debella, E. et al. (2013) Protective role of IL-6 in vascular remodeling in Schistosoma pulmonary hypertension. *Am. J. Respir. Cell Mol. Biol.* **49**, 951–959, https://doi.org/10.1165/rcmb.2012-0532OC

13 Tandrup, T., Gundersen, H.J. and Jensen, E.B. (1997) The optical rotator. *J. Microsc.* **186**, 108–120, https://doi.org/10.1046/j.1365-2818.1997.2070765.x

14 Junqueira, L.C., Bignolas, G. and Brentani, R.R. (1979) Picrosirius staining plus polarization microscopy, a specific method for collagen detection in tissue sections. *Histochem. J.* **11**, 447–455, https://doi.org/10.1007/BF01002772

15 Wang, F., Flanagan, J., Su, N., Wang, L.-C., Bui, S., Nielson, A. et al. (2012) RNAscope: a novel in situ RNA analysis platform for formalin-fixed, paraffin-embedded tissues. *J. Mol. Diagn. JMD* **14**, 22–29, https://doi.org/10.1016/j.jmoldx.2011.08.002
16 Rasband, W.S. *ImageJ*, U. S. National Institutes of Health, Bethesda, Maryland, USA, https://imagej.nih.gov/ij/ 1997-2018
17 Kumar, R., Mickael, C., Chabon, J., Gebreab, L., Rutebemberwa, A., Garcia, A.R. et al. (2015) The causal role of IL-4 and IL-13 in Schistosoma mansoni pulmonary hypertension. *Am. J. Respir. Crit. Care Med.* **192**, 998–1008, https://doi.org/10.1164/rccm.201410-1820OC
18 Kumar, R., Mickael, C., Kassa, B., Sanders, L., Koyanagi, D., Hernandez-Saavedra, D. et al. (2019) Th2 CD4+ T cells are necessary and sufficient for schistosoma-pulmonary hypertension. *J. Am. Heart Assoc.* **8**, e013111, https://doi.org/10.1161/JAHA.119.013111
19 Jarman, E.R., Khambata, V.S., Yun Ye, L., Cheung, K., Thomas, M., Duggan, N. et al. (2014) A translational preclinical model of interstitial pulmonary fibrosis and pulmonary hypertension: mechanistic pathways driving disease pathophysiology. *Physiol. Rep.* **2**, e12133, https://doi.org/10.14814/phy2.12133
20 Rajagopal, K., Bryant, A.J., Sahay, S., Wareing, N., Zhou, Y., Pandit, L.M. et al. (2021) Idiopathic pulmonary fibrosis and pulmonary hypertension: Heracles meets the Hydra. *Br. J. Pharmacol.* **178**, 172–186, https://doi.org/10.1111/bph.15036
21 Thenappan, T., Chan, S.Y. and Weir, E.K. (2018) Role of extracellular matrix in the pathogenesis of pulmonary arterial hypertension. *Am. J. Physiol. Heart Circ. Physiol.* **315**, H1322–H1331, https://doi.org/10.1152/ajpheart.00136.2018
22 Nagai, N., Hosokawa, M., Itohara, S., Adachi, E., Matsushita, T., Hosokawa, N. et al. (2000) Embryonic lethality of molecular chaperone hsp47 knockout mice is associated with defects in collagen biosynthesis. *J. Cell Biol.* **150**, 1499–1506, https://doi.org/10.1083/jcb.150.6.1499
23 Warshamana, G.S., Pociask, D.A., Fisher, K.J., Liu, J.-Y., Sime, P.J. and Brody, A.R. (2002) Titration of non-replicating adenovirus as a vector for transducing active TGF-beta1 gene expression causing inflammation and fibrogenesis in the lungs of C57BL/6 mice. *Int. J. Exp. Pathol.* **83**, 183–201, https://doi.org/10.1046/j.1365-2613.2002.00229.x
24 Barron, L. and Wynn, T.A. (2011) Fibrosis is regulated by Th2 and Th17 responses and by dynamic interactions between fibroblasts and macrophages. *Am. J. Physiol. Gastrointest. Liver Physiol.* **300**, G723–G728, https://doi.org/10.1152/ajpgi.00414.2010
25 Kolosionek, E., Graham, B.B., Tuder, R.M. and Butrous, G. (2011) Pulmonary vascular disease associated with parasitic infection–the role of schistosomiasis. *Clin. Microbiol. Infect. Off. Publ. Eur. Soc. Clin. Microbiol. Infect. Dis.* **17**, 15–24
26 Tuder, R.M., Groves, B., Badesch, D.B. and Voelkel, N.F. (1994) Exuberant endothelial cell growth and elements of inflammation are present in plexiform lesions of pulmonary hypertension. *Am. J. Pathol.* **144**, 275–285
27 Crosby, A., Jones, F.M., Kolosionek, E., Southwood, M., Purvis, I., Soon, E. et al. (2011) Praziquantel reverses pulmonary hypertension and vascular remodeling in murine schistosomiasis. *Am. J. Respir. Crit. Care Med.* **184**, 467–473, https://doi.org/10.1164/rccm.201101-0146OC
28 Crosby, A., Jones, F.M., Southwood, M., Stewart, S., Schermuly, R., Butrous, G. et al. (2010) Pulmonary vascular remodeling correlates with lung eggs and cytokines in murine schistosomiasis. *Am. J. Respir. Crit. Care Med.* **181**, 279–288, https://doi.org/10.1164/rccm.200903-0355OC
29 Crosby, A., Soon, E., Jones, F.M., Southwood, M.R., Haghighat, L., Toshner, M.R. et al. (2015) Hepatic shunting of eggs and pulmonary vascular remodeling in Bmpr2(+/-) mice with Schistosomiasis. *Am. J. Respir. Crit. Care Med.* **192**, 1355–1365, https://doi.org/10.1164/rccm.201412-2262OC
30 Graham, B.B., Bandeira, A.P., Morrell, N.W., Butrous, G. and Tuder, R.M. (2010) Schistosomiasis-associated pulmonary hypertension: pulmonary vascular disease: the global perspective. *Chest* **137**, 20S–29S, https://doi.org/10.1378/chest.10-0048
31 Strahan, R., McAdam, D. and Paul, E. (2020) Change in schistosomiasis-related liver disease with repeated praziquantel treatment in school children in rural Zambia. *Trop. Doct.* **50**, 216–221, https://doi.org/10.1177/0049475520921281
32 Liu, Y., Munker, S., Müllenbach, R. and Weng, H.-L. (2012) IL-13 signaling in liver fibrogenesis. *Front. Immunol.* **3**, 116, https://doi.org/10.3389/fimmu.2012.00116
33 Humbert, M., Guignabert, C., Bonnet, S., Dorfmüller, P., Klinger, J.R., Nicolls, M.R. et al. (2019) Pathology and pathobiology of pulmonary hypertension: state of the art and research perspectives. *Eur. Respir. J.* **53**, 1801887, https://doi.org/10.1183/13993003.01887-2018
34 Stenmark, K.R., Nozik-Grayck, E., Gerasimovskaya, E., Anwar, A., Li, M., Riddle, S. et al. (2011) The adventitia: essential role in pulmonary vascular remodeling. *Compr. Physiol.* **1**, 141–161
35 El Kasmi, K.C., Pugliese, S.C., Riddle, S.R., Poth, J.M., Anderson, A.L., Frid, M.G. et al. (2014) Adventitial fibroblasts induce a distinct proinflammatory/profibrotic macrophage phenotype in pulmonary hypertension. *J. Immunol. Baltim. Md 1950* **193**, 597–609
36 Schäfer, M., Kheyfets, V.O., Schroeder, J.D., Dunning, J., Shandas, R., Buckner, J.K. et al. (2016) Main pulmonary arterial wall shear stress correlates with invasive hemodynamics and stiffness in pulmonary hypertension. *Pulm. Circ.* **6**, 37–45, https://doi.org/10.1086/685024
37 Mori, H., Ishibashi, T., Inagaki, T., Okazawa, M., Masaki, T., Asano, R. et al. (2020) Pristane/Hypoxia (PriHx) mouse as a novel model of pulmonary hypertension reflecting inflammation and fibrosis. *Circ. J. Off. J. Jpn. Circ. Soc.* **84**, 1163–1172, https://doi.org/10.1253/circj.CJ-19-1102
38 Maurer, B., Reich, N., Juengel, A., Kriegsmann, J., Gay, R.E., Schett, G. et al. (2012) Fra-2 transgenic mice as a novel model of pulmonary hypertension associated with systemic sclerosis. *Ann. Rheum. Dis.* **71**, 1382–1387, https://doi.org/10.1136/annrheumdis-2011-200940
39 Zaw, A.M., Sekar, R., Mak, S.O.K., Law, H.K.W. and Chow, B.K.C. (2019) Loss of secretin results in systemic and pulmonary hypertension with cardiopulmonary pathologies in mice. *Sci. Rep.* **9**, 14211, https://doi.org/10.1038/s41598-019-50634-x
40 Kaviratne, M., Hesse, M., Leusink, M., Cheever, A.W., Davies, S.J., McKerrow, J.H. et al. (2004) IL-13 activates a mechanism of tissue fibrosis that is completely TGF-beta independent. *J. Immunol. Baltim. Md 1950* **173**, 4020–4029
41 Ferreira, R., de C. dos, S., Montenegro, S.M.L., Domingues, A.L.C., Bandeira, A.P., Silveira, C.A. et al. (2014) TGF beta and IL13 in Schistosomiasis mansoni associated pulmonary arterial hypertension; a descriptive study with comparative groups. *BMC Infect. Dis.* **14**, 282, https://doi.org/10.1186/1471-2334-14-282

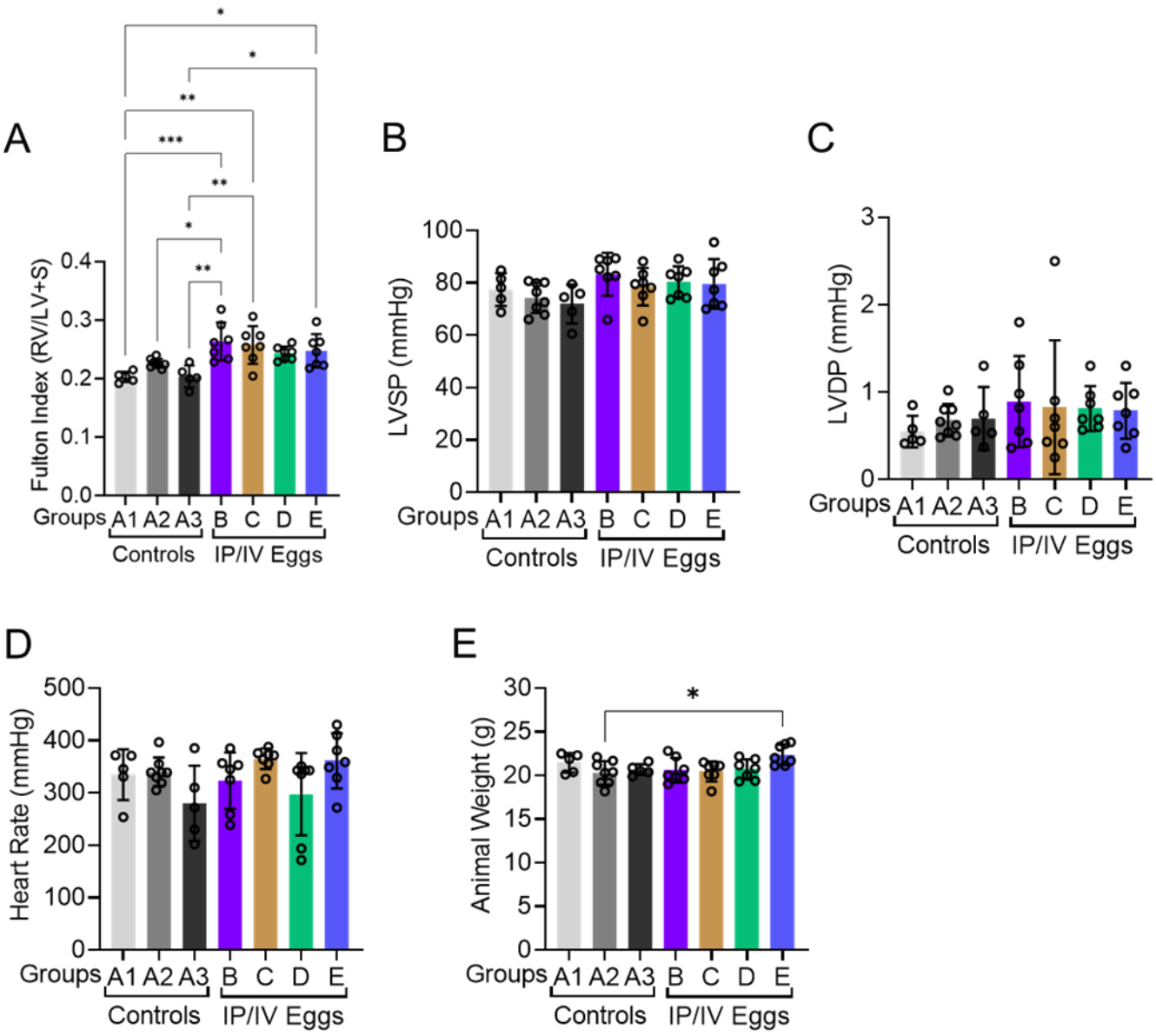

Supplementary Figure 1. The timecourse following a single intravenous dose of *Schistosoma* eggs reveals an increase in right ventricle hypertrophy, but no change in left heart hemodynamics. (A) Right ventricular hypertrophy as measured by Fulton index: the ratio of the mass of the right ventricle (RV) divided by the combined mass of the left ventricle (LV) and septum (S). (B) Left ventricle systolic pressure (LVSP). (C) Left ventricle diastolic pressure (LVDP). (D) Heart rate (HR). (E) Animal body weight. See **Figure 1A** for the group nomenclature. Mean ± SD plotted; analysis of variance (ANOVA) $P<0.001$ for Fulton index with post hoc Tukey tests shown; *$P<0.05$, **$P<0.01$. RV: right ventricle; LV: left ventricle; S: septum; IP: intraperitoneal *Schistosoma* eggs; IV: intravenous *Schistosoma* eggs.

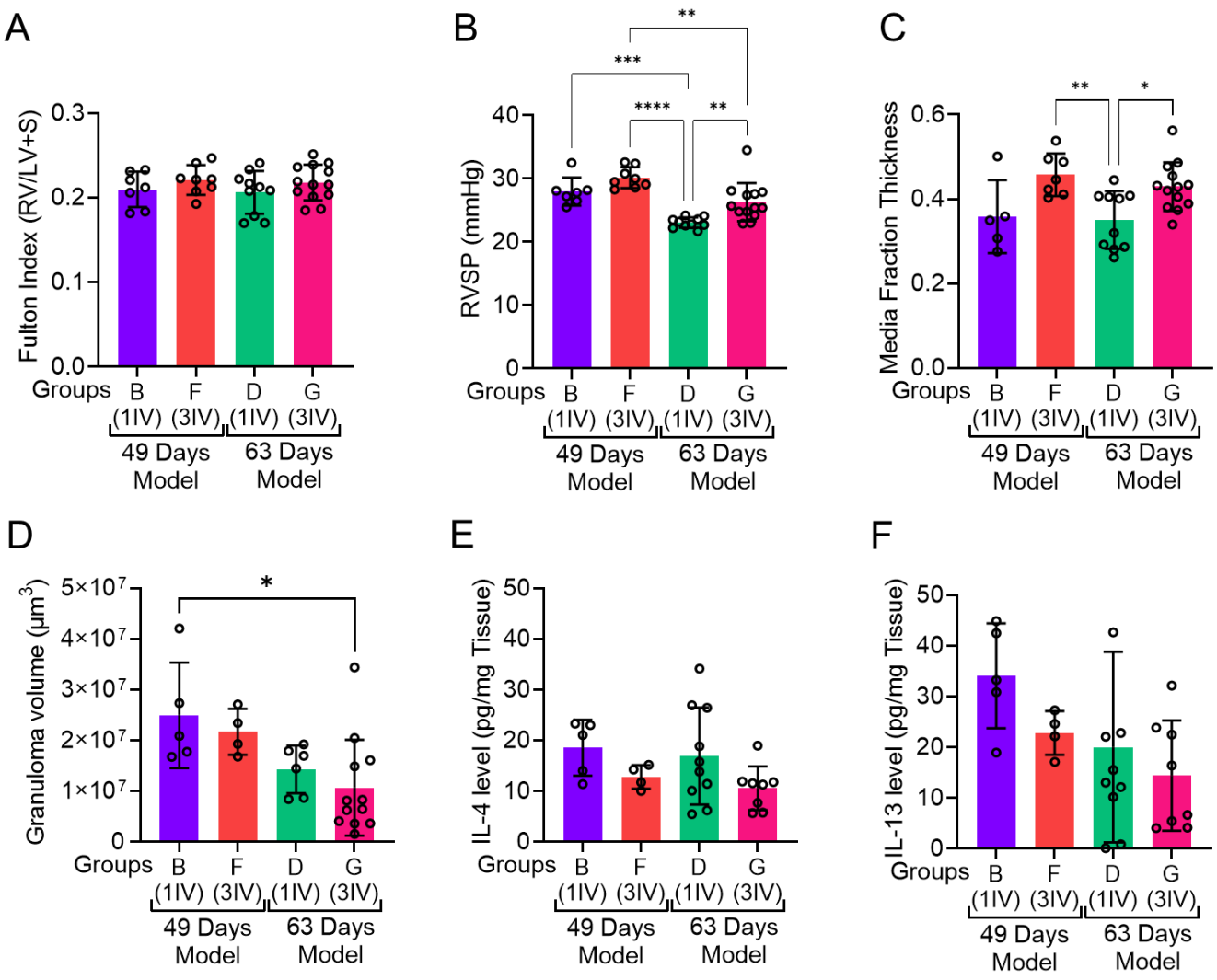

Supplementary Figure 2. Pathology of multiple *Schistosoma* challenged mice. (A) Right ventricular hypertrophy as measured by Fulton index. (B) Right ventricular systolic pressure (RVSP). (C) Quantitative fractional thickness of the pulmonary vasculature. (D) Peri-egg granuloma volumes. (E) IL-4 and (F) IL-13 protein concentrations by ELISA. See **Figures 1A and 2A** for the group nomenclature. Mean ± SD plotted; t tests shown; **P*<0.05, ***P*<0.01, ****P*<0.005, *****P*<0.001. IP: intraperitoneal *Schistosoma* eggs; IV: intravenous *Schistosoma* eggs.)

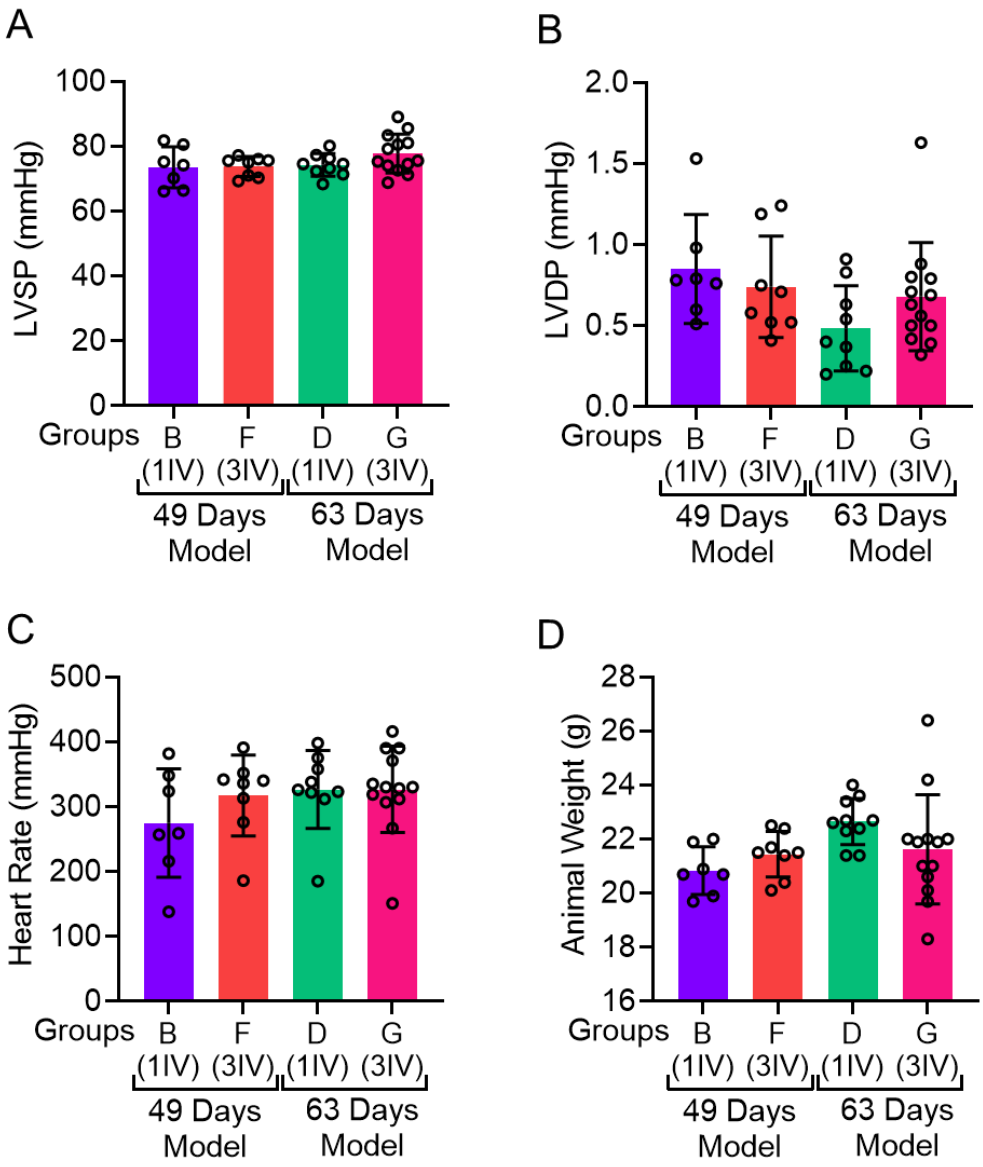

Supplementary Figure 3: The persistent pathology after repeated *Schistosoma* doses is not confounded by changes in left heart hemodynamics or body weight. (A) Left ventricular systolic pressure (LVSP). (B) Left ventricular diastolic pressures (LVDP). (C) Heart rate (HR). (D) Animal body weight. See **Figure 2A** for group nomenclature. Mean ± SD plotted; IV: intravenous *Schistosoma* eggs.

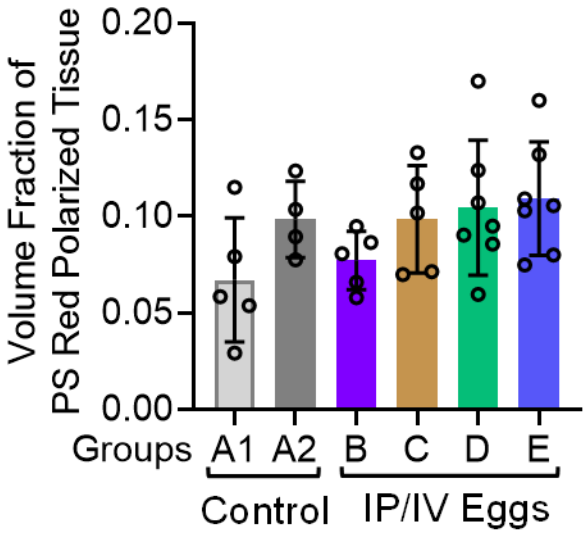

Supplementary Figure 4. No difference in the perivascular collagen as quantified by picrosirus red following a single *Schistosoma* challenge at different timepoints. See **Figure 1A** for group nomenclature; mean ± SD plotted; IP/IV: intraperitoneal/intravenous *Schistosoma* eggs.

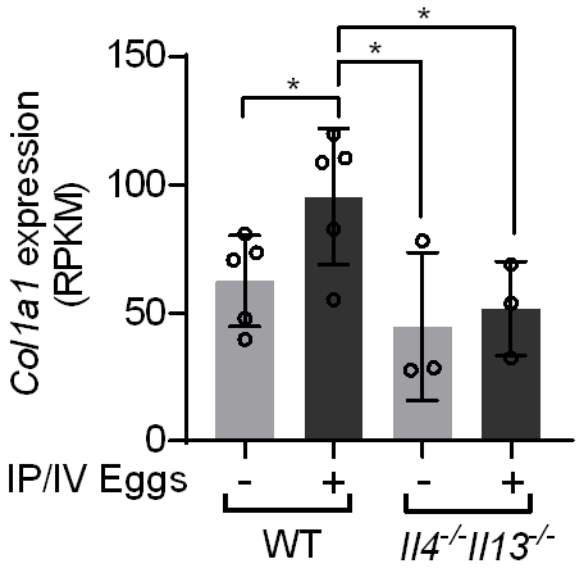

Supplemental Figure 5. Col1a1 mRNA is increased in wildtype mice following *Schistosoma* exposure, which is suppressed in Il4-/-Il13-/- mice. Analysis of previously published (GEO Series accession number GSE49116) mRNA quantification of whole lung lysates for *Col1a1* expression by RNAseq in wildtype (N=5/group) and *Il4*$^{-/-}$*Il13*$^{-/-}$ (N=3/group) mice. Mean ± SD plotted; *: t-test with pairwise comparisons $P<0.05$; IP/IV: intraperitoneal/intravenous *Schistosoma* eggs.

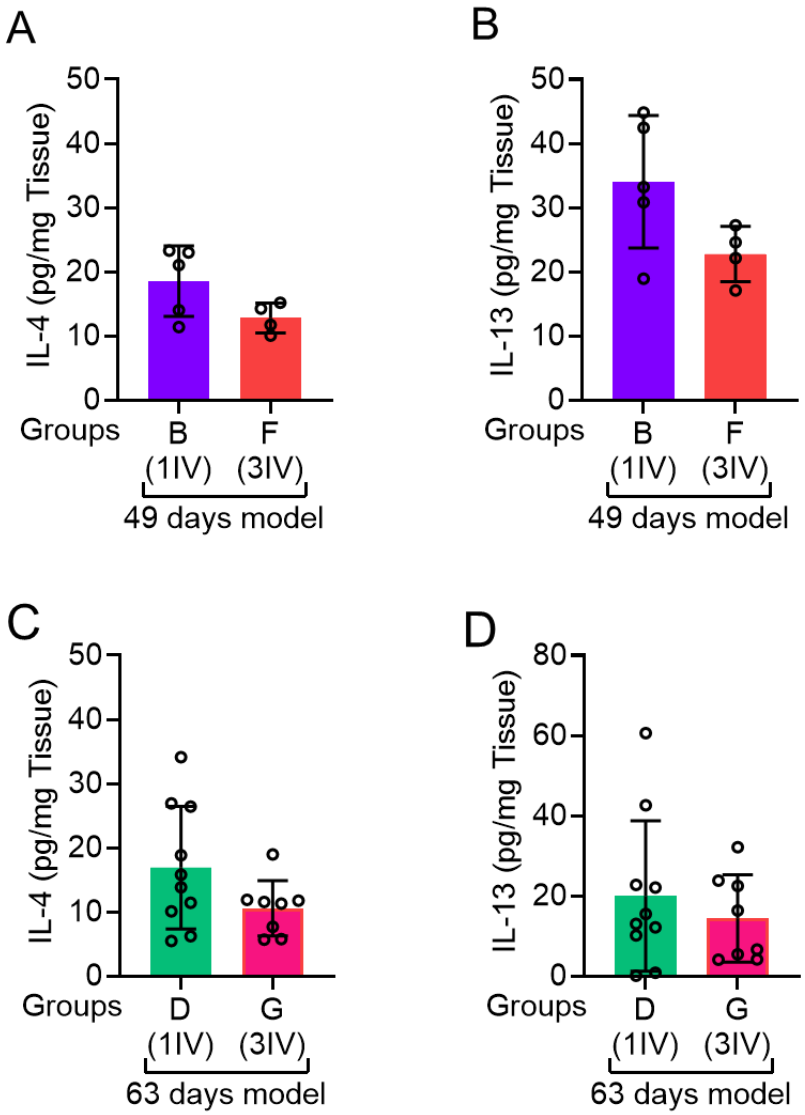

Supplemental Figure 6. IL-4 and IL-13 levels in whole lung lysates are not different between mice singly or multiple challenged with intravenous eggs. (A) IL-4 and (B) IL-13 protein concentrations in whole lung lysates 7d after the final IV eggs, following either 1 or 3 repeated IV egg challenges (*Groups B and F*; N=5-5/group). (C) IL-4 and (D) IL-13 protein concentrations in in whole lung lysates 21d after the final IV eggs, following either 1 or 3 repeated IV egg challenges (*Groups D and G*; N=8-10/group).

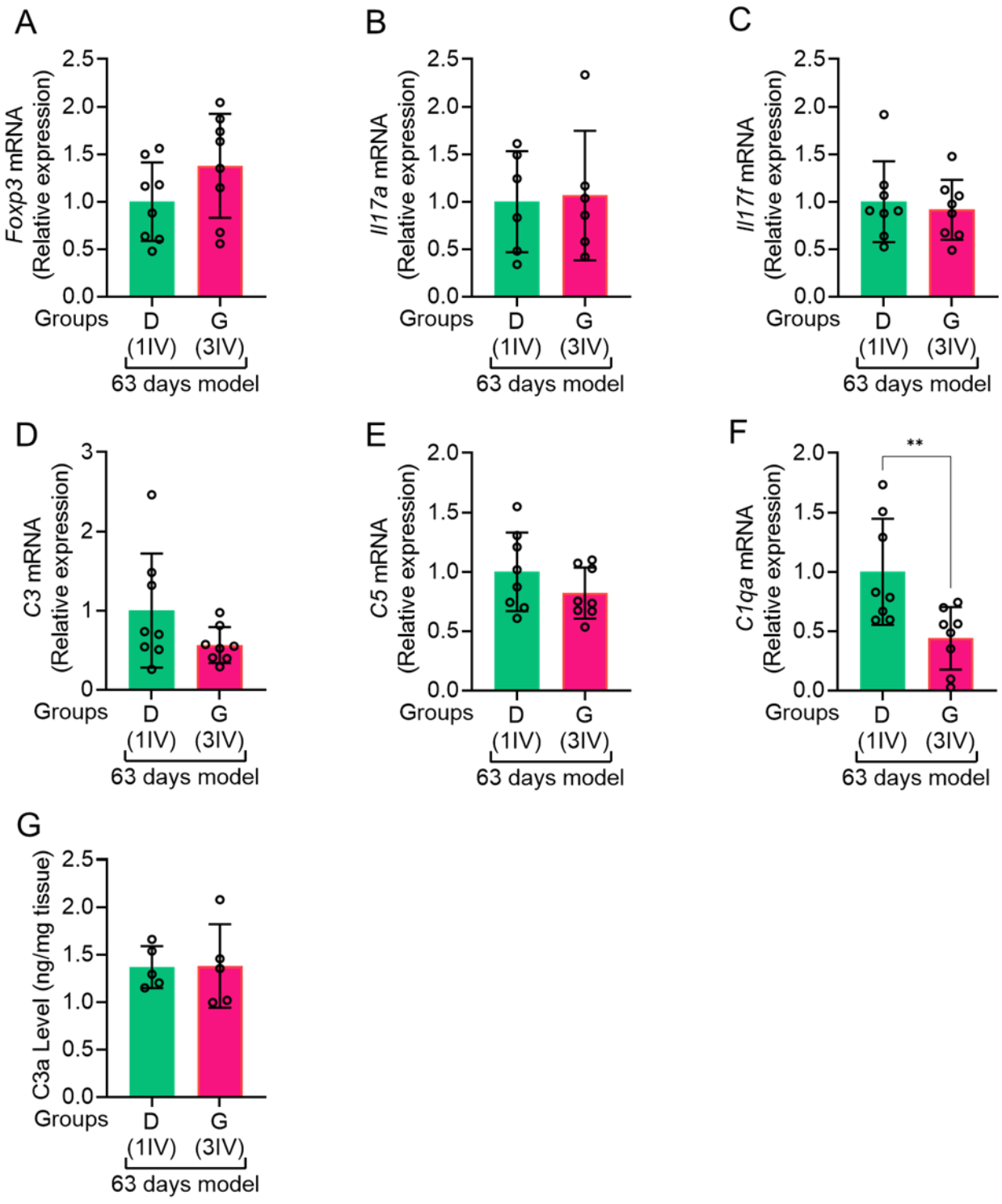

Supplementary Figure 7: The persistent pathology after repeated *Schistosoma* doses is independent of mRNA and protein markers of T cell phenotype and the complement pathway. (A-F) RT-PCR of whole lung lysates; 2-ΔCt method; relative to β-actin housekeeping gene. (A) Foxp3, a marker of Tregs. (B) Il17a and (C) IL17f, markers of Th17 cells. Complement

pathway members (D) C3, (E) C5 and (F) C1qa. (G) ELISA for C3a of whole lung lysates. Mean ± SD plotted; IV: intravenous *Schistosoma* eggs.

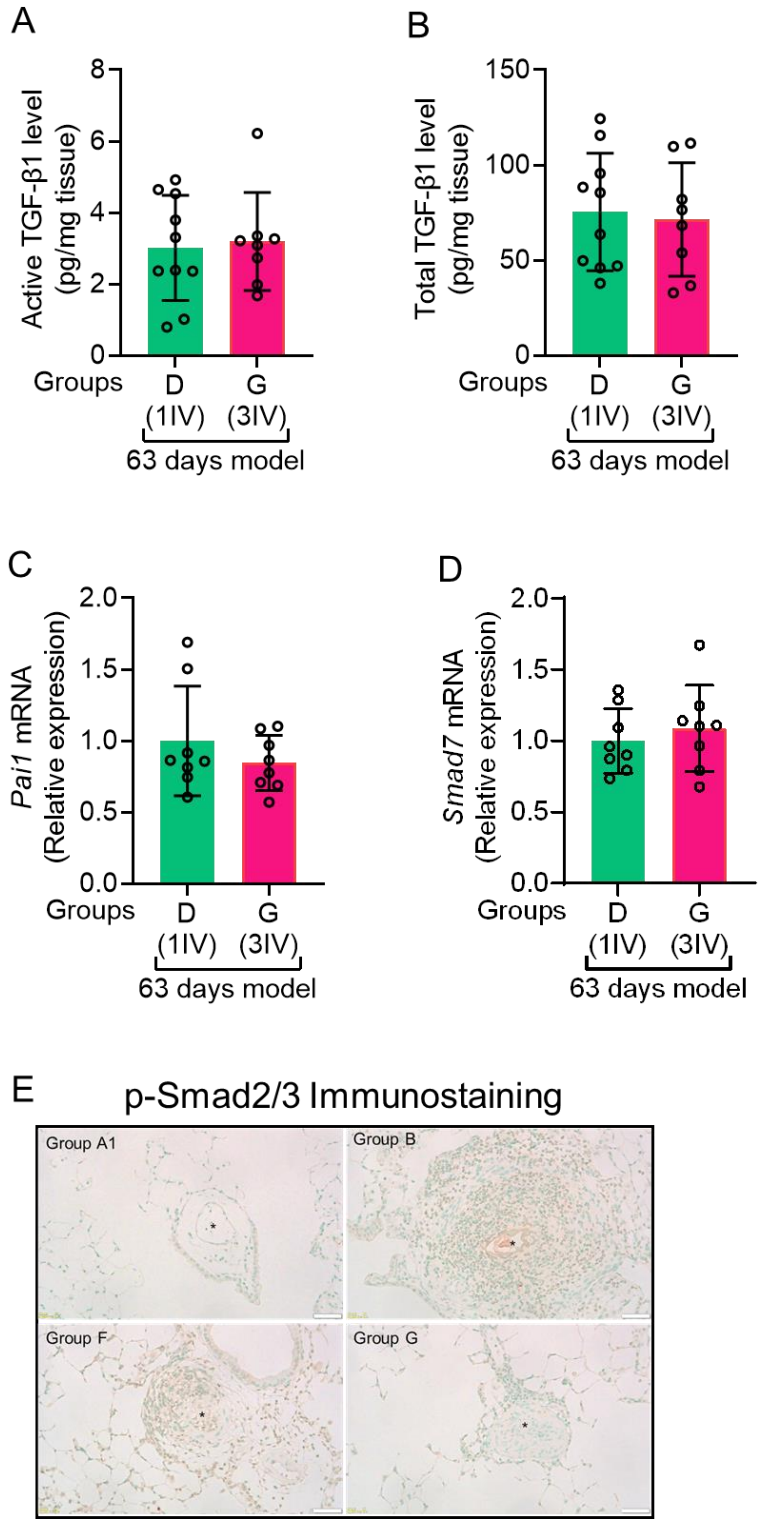

Supplementary Figure 8. The persistent pathology after repeated *Schistosoma* doses is independent of TGF-β signaling. (A) Active and (B) total TGF-β1 in whole lung lysates by ELISA. (C) Pai1 and (D) Smad7 mRNA in whole lung lysates (RT-PCR; $2^{-\Delta Ct}$ method; relative to β-actin housekeeping gene). (E) Immunostain for phospho-Smad2/3, intracellular signaling

mediators of canonical TGF-β signaling. *: vessel lumen. Mean ± SD plotted; IV: intravenous *Schistosoma* eggs.

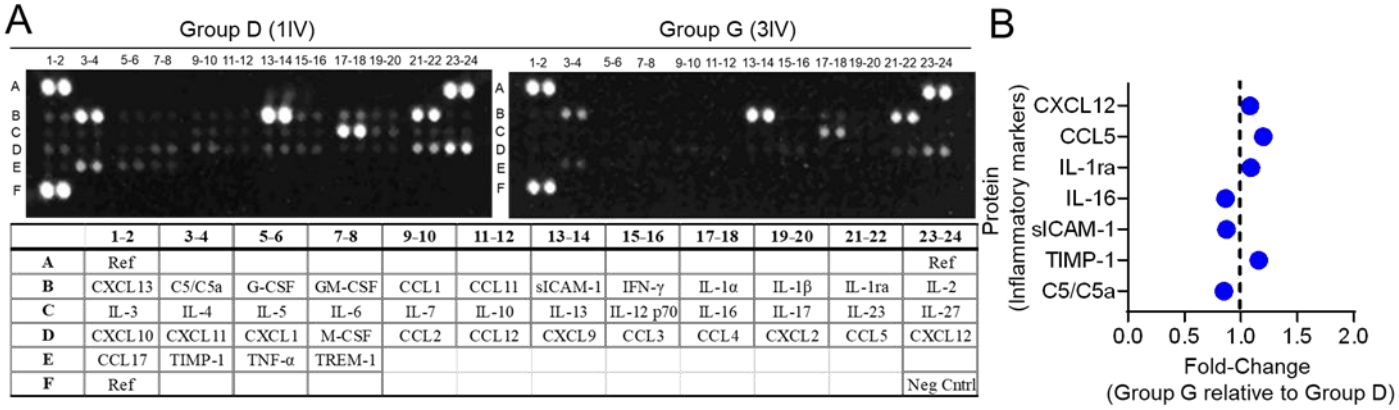

	1-2	3-4	5-6	7-8	9-10	11-12	13-14	15-16	17-18	19-20	21-22	23-24
A	Ref											Ref
B	CXCL13	C5/C5a	G-CSF	GM-CSF	CCL1	CCL11	sICAM-1	IFN-γ	IL-1α	IL-1β	IL-1ra	IL-2
C	IL-3	IL-4	IL-5	IL-6	IL-7	IL-10	IL-13	IL-12 p70	IL-16	IL-17	IL-23	IL-27
D	CXCL10	CXCL11	CXCL1	M-CSF	CCL2	CCL12	CXCL9	CCL3	CCL4	CXCL2	CCL5	CXCL12
E	CCL17	TIMP-1	TNF-α	TREM-1								
F	Ref											Neg Cntrl

Supplementary Figure 9. No significant differences in lung cytokine protein levels between 3 IV challenged versus 1 IV challenged mice. (A) Representative protein arrays for mouse cytokines/chemokines of lung lysates. The table shows the location of analytes on the membrane. (B) Relative expression of cytokines, fold-change of Group G relative to Group D (ratio of means of N=2/group). IV: intravenous *Schistosoma* eggs.

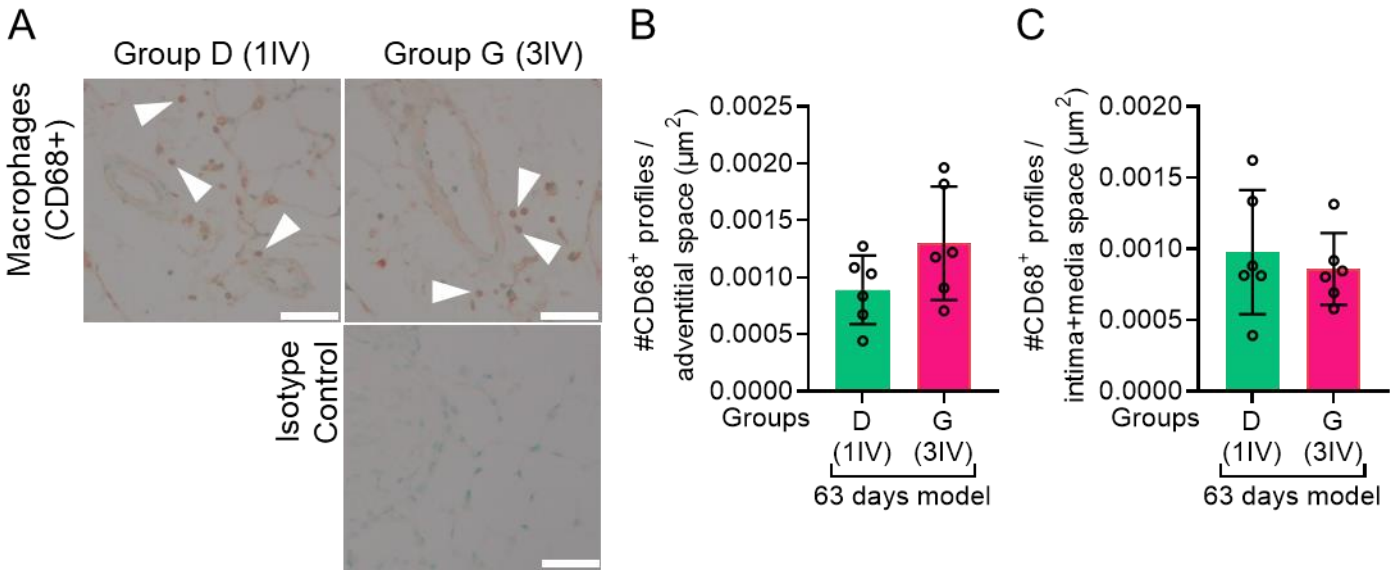

Supplementary Figure 10. No significant differences in the density of CD68-positive cells (macrophages) in the mice that received multiple *Schistosoma* challenges. (A) Representative images of anti-CD68 stain of Groups D and G, and an isotype control. Arrowheads mark CD68-positive cells; scale bars: 50µm. Density of CD68-positive cells in the (B) perivascular/adventitial and (C) intima and media combined (within the adventitia) spaces (N=6/group), *P*=NS for both. Mean ± SD plotted; IV: intravenous *Schistosoma* eggs.

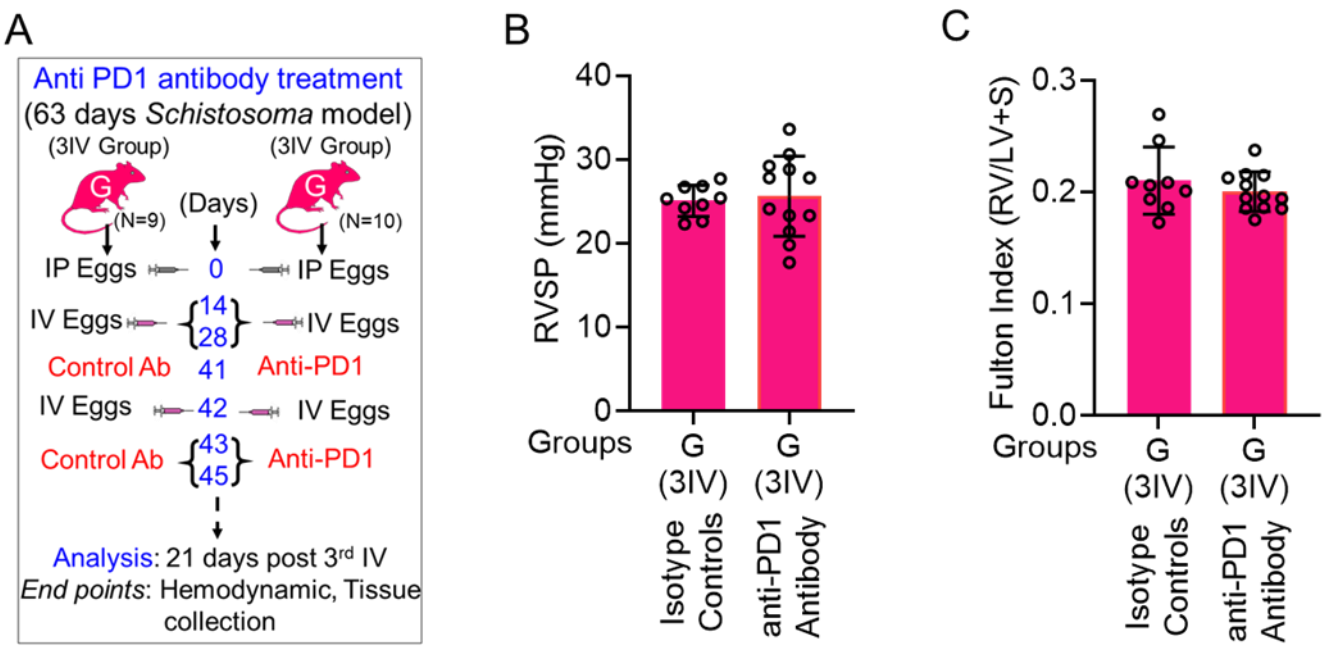

Supplementary Figure 11. Blockade of PD-1 does not attenuate PH pathology in multiple *Schistosoma* challenged mice. (A) Schematic of anti-PD-1 neutralization in *Schistosoma*-exposed mice. (B) Right ventricle systolic pressure (RVSP). (C) RV hypertrophy. Mean ± SD plotted; **P*<0.05, ***P*<0.01, *****P*<0.0001. IP: intraperitoneal; IV: intravenous *Schistosoma* eggs.

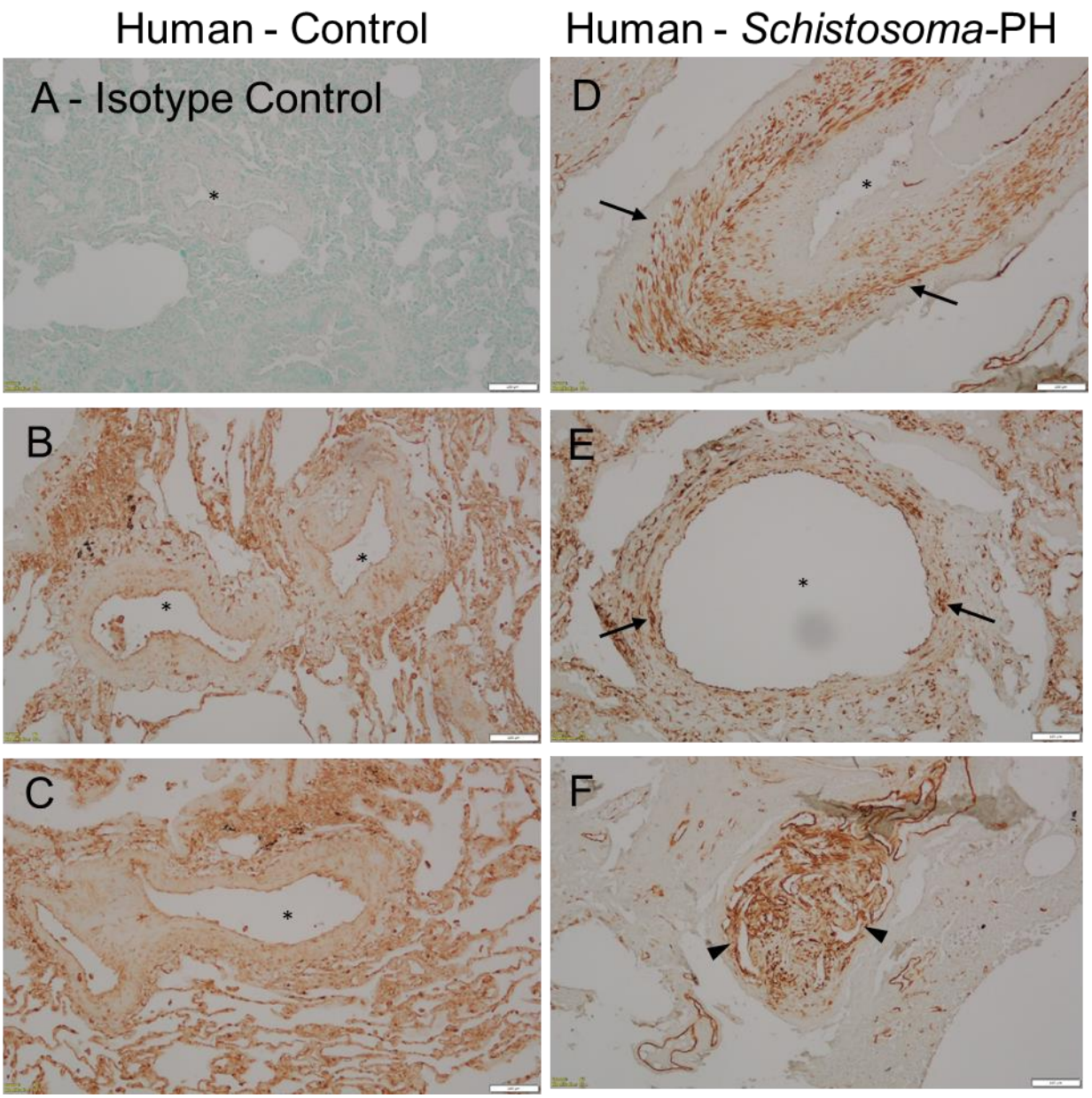

Supplementary Figure 12. Evidence of increased fibroblast density assessed by vimentin staining in the medial vascular compartment in lung tissue from autopsy cases of patients who died of schistosomiasis-associated PH, as compared to control lung tissue. (A) Isotype control of control lung tissue. (B and C) Representative images of vimentin immunostained lung tissue from unsuccessful lung donors. (D and E) Two of three cases of *Schistosoma*-PH analyzed demonstrated substantial vimentin staining in the media. (One of the 4 cases available did not have any significant immunostaining in the entire specimen.) (F) Representative image of a plexiform lesion in *Schistosoma*-PH with significant vimentin immunostaining. *: vessel lumen. Arrows: representative positive staining in the medial compartment. Arrowheads: positive staining in a plexiform lesion. Scale bars: 100 μm.

Supplemental Table 1. Primers used for mouse mRNA quantification by RT-PCR.

All primers are TAQMAN Gene Expression Assays (Life Technologies Corporation, Carlsbad, CA, USA).

Target	Catalog #	Interrogated Sequence	Amplicon Length
Pai1	Mm00435858_m1	NM_008871.2	87
Smad7	Mm00484742_m1	NM_001042660.1	119
Foxp3	Mm00475157_g1	NM_054039.2	87
Thbs1	Mm01335413_g1	NM_011580.3	84
Il17a	Mm00439618_m1	NM_010552.3	80
Il17f	Mm00521423_m1	NM_145856.2	85
C3	Mm01232779_m1	BC029976.1	88
C5	Mm00439275_m1	NM_010406.2	104
C1qa	Mm00432142_m1	NM_007572.2	80
Actb	Mm02619580_g1	AK075973.1	143
Gapdh	Mm99999915_g1	NM_008084.3	107
Pdcd1 (PD1)	Mm00435532_m1	NM_008798.2	65
Cd274 (PDL1)	Mm00452054_m1	NM_021893.3	77
Pdcd1lg2 (PDL2)	Mm00451734_m1	NM_021396.2	95

Supplemental Table 2. Reagents for immunostaining mouse tissue. All rinses between steps in TBST unless noted otherwise.

Immunostain	Antigen Retrieval	Block	Primary Antibody	Secondary Antibody	Tertiary Reagent
αSM-actin	Citrate Buffer 20 min in steamer (Vector H-3300)	Avidin 10 min, Biotin 10 min, Mouse on Mouse (MOM) kit blocking solution (Vector BMK-2202) 1hr at RT	1:100 30min at RT (Dako #M0851)	MOM Biotinylated anti-Mouse Reagent (Vector BMK-2202) 10min at RT	Texas Red-Strepavidin 1:2000 (Invitrogen #S872), Vectashield with DAPI (Vector H-1500)
p-Smad2/3	Borg Decloaker RTU (BioCARE MEDICAL BD1000G1)	10% Goat Serum in TBS 1hr at RT	1:200 1hr at RT (Thermo-Fisher #PA5-99378)	1:200 Goat anti-Rabbit in TBS 1hr at RT (Vector BA-1000)	SA-HRP 30min (Vector SA-5704), DAB 5min at RT (Vector, SK-4100), Methyl Green Counterstain (Vector H3402)
HSP47	Borg Buffer 20 min in steamer (Biocare Borg Decloaker)	Avidin 10 min, Biotin 10 min, 3% H_2O_2 in PBS (5min), Endogenous Enzyme Block (5min; Dako S2003), 10% goat serum in PBS 1hr at RT	1:500 1hr at RT (Abcam ab254015)	1:200 Biotinylated Goat anti-Rabbit (Vector BA-1000)	
CD68	Citrate Buffer 20 min in steamer (Vector H-3300)		1:100 1hr at RT (Invitrogen #PA5-89134)		

Supplemental Table 3. Reagents for immunostaining human tissue. All rinses between steps in TBST unless noted otherwise.

Immunostain	Antigen Retrieval	Block	Primary Antibody	Secondary Antibody	Tertiary Reagent
Vimentin	Borg Buffer 20 min in steamer (Biocare Borg Decloaker)	3% H_2O_2 in PBS (5min), Endogenous Enzyme Block (5min; Dako S2003)	1:500 in PBS 1hr at RT (abcam ab92547)	Anti-Rabbit poly-HRP (Dako EnVision+ K4003)	DAB 5min at RT (Vector, SK-4100), Methyl Green Counterstain (Vector H3402)

Supplemental Table 4. Demographic data on the control human specimens (N=3). (Data on the schistosomiasis-associated pulmonary arterial hypertension specimens was not available.)

Age	Median = 45, Range 27 – 55
Sex	2 Female, 1 Male
Race	3 White